Morphological and Isotopic Changes of *Anabaena cylindrica* PCC 7122 in Response to N_2 Partial Pressure

A Thesis Submitted to the Honors Council of the College of Arts and Sciences of the University of Colorado, Boulder in Partial Fulfillment of Departmental Honors Graduation

Thesis Advisors: Dr. Sebastian Kopf
Dr. Sanjoy Som
Committee Members: Dr. Jennifer Martin
Dr. Heidi Day

Department of Molecular, Cellular and Developmental Biology

Shaelyn Silverman

April 4th, 2017

TABLE OF CONTENTS

CHAPTER ONE

Introduction and Background

The famous space race of the mid-1900s captivated the world for decades and left a profound legacy. Now, a second revolution in space exploration is underway, this time extending beyond the outer reaches of our Solar System. Since the dawn of the first discovery of extrasolar planets (exoplanets) in the 1990s, our ability to detect and characterize these planets has advanced tremendously, in part due to the success of the Kepler Space Telescope. Though humanity may be far from answering the daunting question, "Are we alone?", we can begin to advance toward this goal by assessing whether these exoplanets are habitable. By our unavoidably anthropocentric definition, a habitable planet should be terrestrial, sustain liquid water and hold an atmosphere, albeit this definition is flexible. The composition of a planet can be inferred from knowledge of the planet's mass and volume, and the ability of a planet to sustain liquid water can be deduced from the planet's orbital distance from its parent star. While these are all calculable properties, the ability of an exoplanet's atmosphere to provide insight into whether the planet may be inhabited is less straightforward and is further limited by our knowledge of only a single habitable atmosphere: that of Earth.

The major constituents of Earth's atmosphere today, N_2 (0.79 bar) and O_2 (0.21 bar), greatly contribute to the planet's habitability. Despite the fact that this composition has fluctuated substantially over geological time (Som et al., 2016; Holland, 2006; Marty et al., 2013), Earth has supported life for at least 3.5 billion years (Schopf, 1993; Dodd et al., 2017). Thus, obtaining "snapshots" of Earth's atmosphere over

geological time can greatly enlarge our current database of known habitable atmospheres. At any time point in Earth's history, an upper limit can be placed on the partial pressure of possible atmospheric constituents by knowledge of the total atmospheric pressure, and likewise, knowledge of any constituent's partial pressure places a lower limit on the total atmosphere. Constraining absolute atmospheric pressure is a tremendously difficult feat because an atmosphere leaves a nearly imperceptible physical imprint in the rock record (Som et al., 2016). Attempts at assessing the partial pressure of individual atmospheric constituents are usually based on their biogeochemical implications and imprints in the rock record, such as banded iron-formations (Cloud, 1973), which is only possible for chemically reactive gases. Here, we focus on possible constraints on the N_2 partial pressure (pN_2) (summarized in Fig. 1) as nitrogen gas is chemically almost completely inert yet at the same time a crucial element for life, and fluctuation of its atmospheric levels may be a strong diagnostic for inhabited terrestrial planets (Stüeken et al., 2016). In particular, $N_2/^{36}Ar$ ratios in fluid inclusions trapped in quartz indicated that the partial pressure of N_2 may have been as low as 0.5 bar with an upper limit of 1.1 bar 3.0-3.5 billion years ago (Ga) (Marty et al., 2013). An upper limit of 0.23 ± 0.23 (2σ) bar has been placed on air pressure 2.7 Ga from analysis of lithified gas bubbles in basaltic lava flows (Som et al., 2016), which challenges the theory that higher N_2 levels kept Earth sufficiently warm 2.5 Ga through pressure broadening despite the lower energy output of the Sun during the Faint Young Sun period (Goldblatt et al., 2009). Earth's pN_2 appears to have remained roughly 0.78 bar for the last 600 million years, as indicated by the N/C ratio of sedimentary organic matter (Berner, 2006). Our limited techniques for measuring

ancient air pressure necessitates the search for additional proxies that can enable us to further constrain measurements at these time points and other periods of Earth's history.

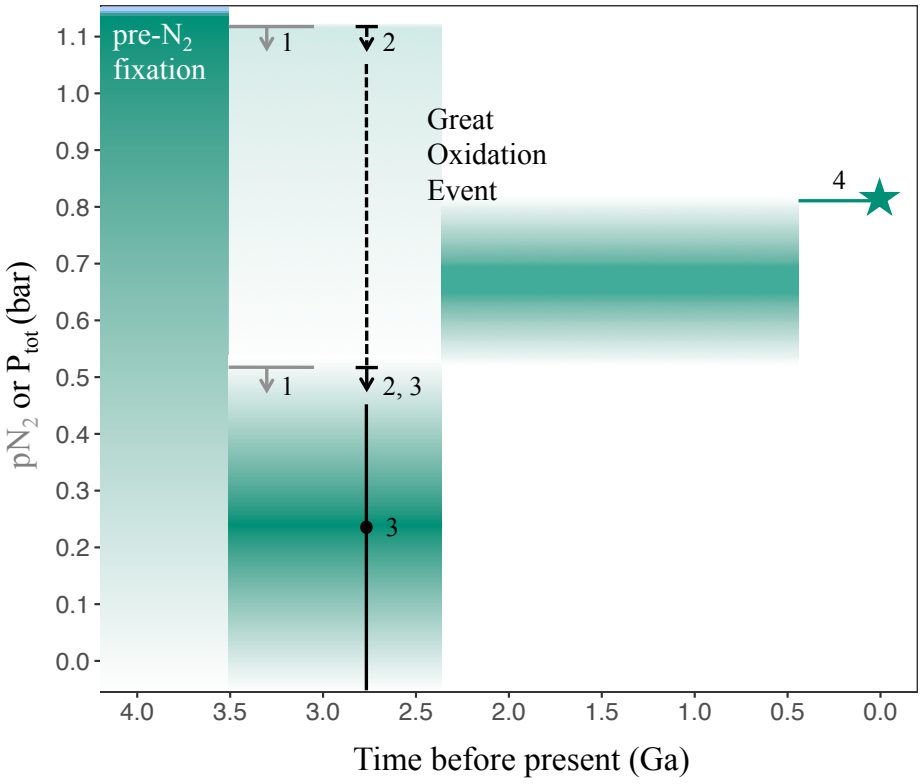

Figure 1. Current estimates for atmospheric N_2 levels throughout Earth's history. Darkly shaded regions indicate a higher degree of certainty to which these measurements have been constrained, and measurements beyond 2.4 Ga are presented as upper limit estimates, denoted by solid lines. Constraints are heavily data-limited, but overall pN_2 appears to have fluctuated in a U-shaped trend. Graph compiled by data from [1]Marty et al. (2013), [2]Som et al. (2012), [3]Som et al. (2016) and [4]Berner (2006).

The coevolution of Earth's atmosphere and biosphere over geological time offers the possibility for microbial species to reveal a wealth of knowledge about Earth's history if properly exploited. In particular, cyanobacteria are among the oldest microorganisms on Earth, having existed for at least 2.35 billion years (Kopp et al., 2005; Ward et al., 2015), possibly even 2.7 Ga (Buick, 2008). Formerly referred to as

"blue-green algae" (all other algae are eukaryotic), these gram-negative photosynthetic bacteria predominantly inhabit marine environments (Fogg et al., 1973). They are the evolutionary ancestors of chloroplasts used in eukaryotic photosynthesis, and may have been responsible for dramatically increasing the oxygen content in our atmosphere ~2.4 Ga ago, during a major biogeochemical transition of the Earth surface environment commonly referred to as the Great Oxidation Event (Schopf and Walter, 1982; Kopp et al., 2005; Kump, 2008). In addition, cyanobacteria contribute the largest flux of new nitrogen to Earth's ecosystems through their ability to convert inorganic N_2 to organic nitrogen in a process known as nitrogen fixation (Fay, 1980).

Among the multitude of cyanobacteria groups, organisms of the filamentous genera *Anabaena* are of particular interest as potential pN_2 proxies because they can overcome nitrogen limitation in their environment by developing specialized cells known as heterocysts that fix N_2 into bioavailable forms of nitrogen and laterally distribute it to neighboring cells along the one-dimensional filaments (Kumar et al., 2010; Golden and Yoon, 2003; Fay, 1992; Gordon and Gordon, 2016). Nitrogen fixation and heterocyst differentiation are two energetically expensive processes, so it is likely that the physiological mechanism controlling the location and number of heterocyst differentiations in *Anabaena* species evolved to ensure the minimum number of heterocysts necessary to satisfy the filaments' nitrogen requirements. Considering this, we develop the hypothesis suggested by Richard Gordon (personal communication, 2015) that the distance between adjacent heterocysts along a filament is a reflection of dissolved concentration of aqueous N_2, which directly correlates with atmospheric N_2 partial pressure by Henry's law (Sander, 2015) assuming equilibrium conditions

between the aqueous and gaseous phases. The actual reduction of N_2 to ammonia (NH_3) during nitrogen fixation is catalyzed by the highly specialized enzyme nitrogenase, which is localized to the heterocysts. We further hypothesize that the dissolved concentration of aqueous N_2 (and thereby the overlying atmospheric partial pressure) modulates the substrate availability for nitrogenase and thereby alters its effective isotopic signature.

In the following thesis, I thus present the results of studies addressing the hypotheses that:

1) pN_2 is reflected in the morphological signature of heterocysts in *Anabaena cylindrica* and *Anabaena variabilis*
2) pN_2 is reflected in isotopic signature of nitrogen fixation by *Anabaena cylindrica*

If correct, then these organisms (and more broadly cyanobacteria) provide a possible proxy for measuring atmospheric N_2 levels, which could contribute new geobarometers that would complement existing methods of quantifying ancient nitrogen partial pressure. The viability of these applications for this purpose is discussed in the final chapter.

CHAPTER TWO

Heterocyst Pattern Formation Responds to N_2 Partial Pressure in *Anabaena cylindrica* PCC 7122 but not in *Anabaena variabilis* ATCC 29413

Abstract

Many filamentous cyanobacteria overcome nitrogen limitation by developing heterocysts, specialized cells that maintain microoxic environments to protect the oxygen-sensitive nitrogen-fixing enzyme nitrogenase. Under current atmospheric conditions (0.79 bar N_2, 0.21 bar O_2), heterocysts form in a well-regulated pattern along the filaments with a separation distance of about 10 to 20 vegetative cells that is maintained as the cells divide. Previous attempts to understand this developmental pattern have focused on the control by genetic expression and nitrogen bioavailability, but no study has examined whether heterocyst development is influenced by the availability of N_2, which scales directly with atmospheric N_2 partial pressure (pN_2) by Henry's law. Here I have investigated whether pN_2 affects heterocyst spacing in two cyanobacterial species. In *Anabaena cylindrica* PCC 7122 filaments, heterocyst spacing appears to be regulated by N_2 through its effect on the nitrogen fixation rate. In contrast, it is unclear whether the heterocyst pattern in *Anabaena variabilis* ATCC 29413 responds to pN_2.

Introduction

In addition to oxygen-evolving photosynthesis, many species of cyanobacteria are capable of nitrogen fixation and will do so in the absence of bioavailable nitrogen (such as nitrate, ammonium and organic nitrogen) to satisfy their nitrogen requirements. However, nitrogenase, the enzyme that facilitates nitrogen fixation (Fig. 2), is extremely sensitive to oxygen, so cyanobacteria have evolved the ability to separate nitrogen fixation from photosynthesis either temporally or spatially. *Anabaena cylindrica* and *Anabaena variabilis* are part of a group of heterocyst-forming cyanobacteria that differentiate these highly specialized cells, which maintain anaerobic microenvironments to protect nitrogenase from oxygen. Here I provide a brief review of nitrogenase and heterocyst formation before proceeding to the main discussion.

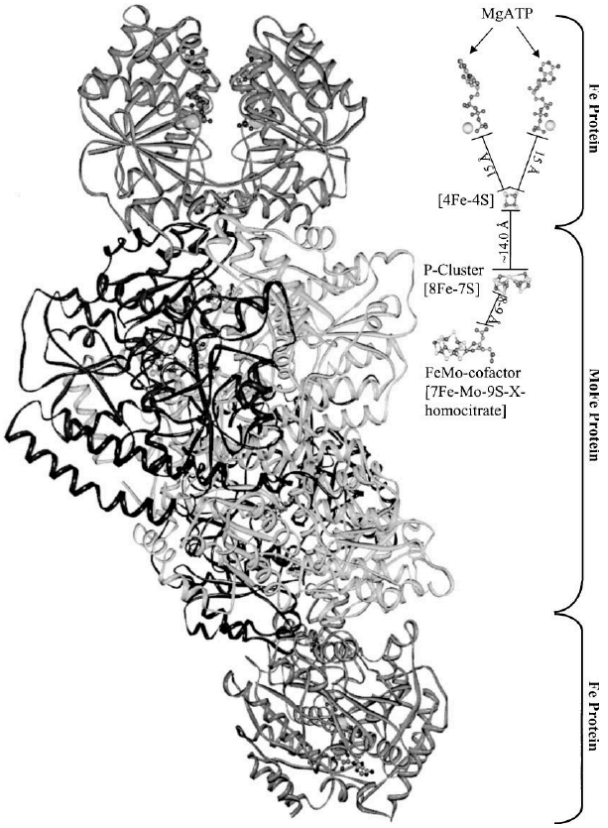

Figure 2. Structure of the Mo-dependent nitrogenase (the major isoenzyme responsible for nitrogen fixation in cyanobacteria) as determined by X-ray crystallography. The dinitrogenase component (middle) consists of one MoFe protein, while the azoferredoxin component (top and bottom) consists of two identical Fe protein subunits. Azoferredoxin is believed to transfer electrons to dinitrogenase by hydrolyzing MgATP to MgADP. Image originally found in Igarishi and Seefeldt (2003).

Nitrogenase

The synthesis of nitrogenase is initiated when vegetative cells become starved of biological nitrogen beyond a threshold (Fleming and Haselkorn, 1973). This enzyme is composed of two subunits: dinitrogenase and dinitrogenase reductase (also known as azoferredoxin) that each carry out important roles in nitrogen fixation (Fay, 1992). Dinitrogenase catalyzes the main nitrogen fixation reaction, the breaking of the extremely stable N≡N triple bond and reduction to ammonia (NH_3), while azoferredoxin supplies the necessary electrons for this reduction to the dinitrogenase active site (Beaumont et al., 2000). In N_2 fixation, one molecule of N_2 is reduced to produce two molecules of ammonia (NH_3) in the following net reaction (Gallon, 1992):

$$N_2 + 8H^+ + 8e^- \rightarrow 2NH_3 + H_2 \quad (1)$$

In this process, approximately 16 ATPs are consumed, rendering nitrogen fixation an energetically expensive process. The most common form of the dinitrogenase enzyme contains a Fe and Mo metal cofactor, but two other isozymes exist that are Fe-Fe or Fe-V proteins (Ward, 2012; Fay, 1992). In contrast, azoferredoxin only contains Fe (Fay, 1992). The nitrogenase complex as a whole, which consists of dinitrogenase and azoferredoxin, is named according to which of the variable metals it contains (i.e. “Mo-nitrogenase”, “V-nitrogenase” or “Fe-nitrogenase”). Because these metalloenzymes are inactivated by oxygen (Burris et al., 1980; Mortenson and Thorneley, 1979; Robson and Postgate, 1980), some cyanobacteria, including *Anabaena*, have evolved the ability to differentiate heterocysts, which spatially separate the two incompatible processes occurring within cyanobacterial cells: oxygen-producing photosynthesis and oxygen-sensitive nitrogen fixation.

Most *Anabaena* species possess a single *nif* ("nitrogen fixing") gene cluster that encodes the components of the nitrogenase complex (Fay, 1992). *A. cylindrica*, in particular, is thought to only synthesize a Mo-nitrogenase (Attridge and Rowell, 1997). In contrast, *A. variabilis* possesses three sets of nitrogenase genes: two encoding Mo-nitrogenases (Brusca et al., 1989; Herrero and Wolk, 1986; Thiel et al., 1997; Thiel et al., 1995) and one encoding a V-nitrogenase (Thiel et al., 1997). The Mo-nitrogenases are independently expressed by the genes *nif1* in heterocysts under oxic conditions (Brusca et al., 1989; Herrero and Wolk, 1986) and by *nif2* in vegetative cells under anoxic conditions (Elhai and Wolk, 1990; Thiel et al., 1995). In contrast, the V-dependent nitrogenase is encoded by the *vnf* cluster and is expressed in *A. variabilis* cells starved of molybdenum (Thiel et al., 1997; Thiel et al., 1995; Thiel, 1993).

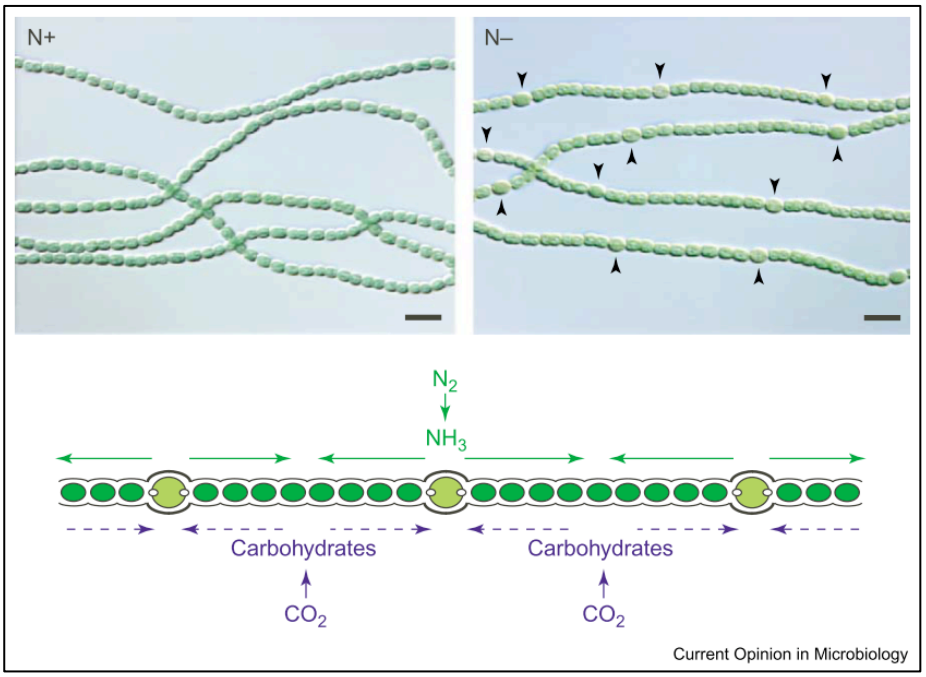

Figure 3. *Anabaena* PCC 7120 develop heterocysts (indicated by arrowheads) in absence (N–) of bioavailable nitrogen, but not in presence (N+). Heterocysts supply vegetative cells with fixed nitrogen in the form of amino acids (Thomas et al., 1977), and in turn, vegetative cells provide heterocysts with fixed carbon (Wolk, 1968). Image taken from Golden and Yoon (2003).

Heterocysts

Heterocysts provide localized microoxic environments in which nitrogenase can operate (Figs. 3 and 4). During differentiation from vegetative cells, heterocysts undergo a series of structural and biochemical changes that serve to minimize the amount of oxygen present inside the cell. As a first barrier of protection, heterocysts possess an outer polysaccharide layer and inner glycolipid layer composed of unique glycolipids specific to heterocysts (Winkenbach et al., 1972; Wolk and Simon, 1969) (Fig. 4), which both contribute to their thick cellular walls (Lang and Fay, 1971). Together, the layers limit the rate of gas diffusion into the heterocysts (Lambein and Wolk, 1973; Murry and Wolk, 1989; Wolk et al., 1988), thus minimizing oxygen entry (Haury and Wolk, 1978; Hallenbeck et al., 1979; Buikema and Haselkorn, 1991). Symbiotic bacteria surrounding heterocysts, eliminated in this study, also help create an anoxic environment for the heterocyst (Paerl, 1978). Despite these barriers, heterocysts are not completely impermeable to oxygen (Walsby, 1985), so they have high respiration rates (Fay and Cox, 1967; Fay, 1992) to maintain the near-anaerobic conditions required to protect nitrogenase. As an additional mechanism to limit oxygen entry, the plasma membranes of heterocysts and neighboring vegetative cells converge into narrow pores traversed by hundreds of microplasmodesmata (Lang and Fay, 1971; Giddings and Staehelin, 1981) (Fig. 4), which also serve to increase the intercellular transport network (Fay, 1992; Haselkorn, 1978). N_2 gas is believed to enter the heterocysts through either these pores, or through the periplasm, an intrafilamentous route continuous across vegetative and heterocystous cells (Walsby, 2007).

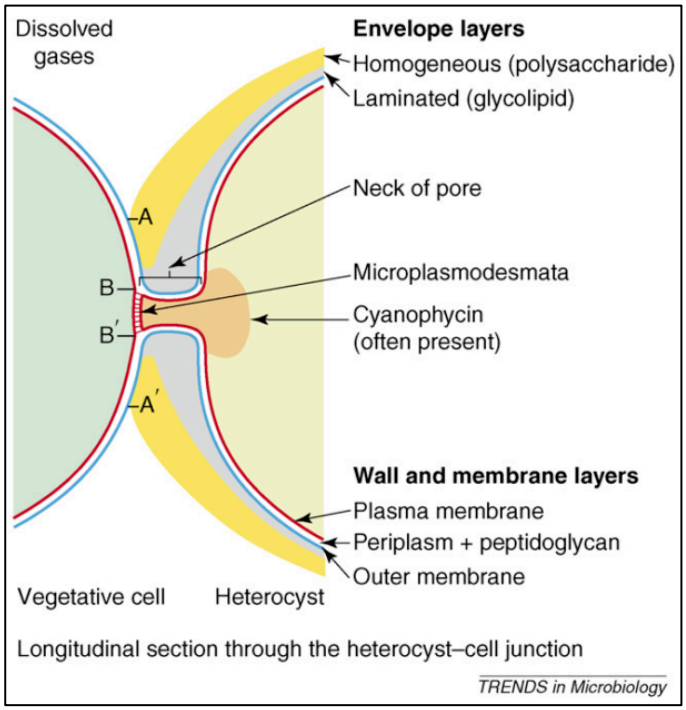

Figure 4. Structural features of the heterocyst-vegetative cell junction. The heterocyst envelope is composed of two outer polysaccharide layers and one inner glycolipid layer (Cardemil and Wolk, 1979; Buikema and Haselkorn, 1991), which all serve to limit O_2 entry. Fixed nitrogen reserves are stored in cyanophycin at the polar region of heterocysts (Wolk et al., 1994). N_2 gas may enter the heterocyst either through the pore (area B,B') traversed by microplasmodesmata, or through the periplasmic space (white) between the outer and plasma membrane. Figure produced by Walsby (2007).

Biochemical changes within heterocysts that help reduce oxygen production include degradation of 17 of the 35 majors proteins found in vegetative cells during the initial stages of heterocyst development (Fleming and Haselkorn, 1974; Wood and Haselkorn, 1976). Among these are enzymes that facilitate carbon fixation (Codd and Stewart, 1977; Winkenbach and Wolk, 1973), such as ribulose bisphosphate carboxylase (rubisco), which is involved in the first step of carbon fixation in photosynthesis. The photosystem II protein complex is also degraded (Donze et al., 1972; Tel-Or and Stewart, 1975; Thomas, 1970), as well as the photosystem II-associated phycobiliproteins, which transfer light energy to chlorophyll *a* (Glazer,

1987). Lack of these components contributes to the heterocysts' inability to carry out water-splitting photosynthesis, which abolishes intracellular oxygen production. However, heterocysts retain the photosystem I complex (Donze et al., 1972; Stewart et al., 1975; Tel-Or and Stewart, 1977), enabling the continued production of ATP from cyclic photophosphorylation to carry out necessary metabolic cellular functions (Haselkorn and Buikema, 1992).

Nitrogenase requires a continuous supply of carbon (Wolk, 1968), which serves as a source of both energy and reductant for nitrogen fixation (Fay, 1992). Heterocysts cannot photosynthesize, so vegetative cells supply heterocysts with fixed carbon, and in return, heterocysts transport fixed nitrogen to the vegetative cells as amino acids (Fig. 3; Meeks et al., 1978). This exchange of molecules is thought to take place via passive diffusion along the periplasm (Flores et al., 2006).

Mechanism of heterocyst differentiation

2-oxoglutarate

The deficiency of bioavailable forms of nitrogen triggers several pathways that ultimately cause vegetative cells to differentiate into heterocysts. A simplified visual summary of these pathways is provided in Figure 5. Within one hour following nitrogen limitation, vegetative cells experience an intracellular buildup of 2-oxoglutarate (2-OG), an intermediate of the citric acid cycle that is normally converted to succinyl-CoA by the enzyme 2-oxoglutarate dehydrogenase. However, because cyanobacteria lack this enzyme (Laurent et al., 2001; Stanier and Cohen-Bazire, 1977), 2-OG instead serves as the carbon backbone for ammonium incorporation in the glutamine synthetase-

glutamate synthase (GS-GOGAT) cycle in which enzymes catalyze the conversion of 2-OG and ammonia to glutamate, thereby providing a precursor for many amino acids required by the cells (Temple et al., 1998). This step importantly connects carbon and nitrogen metabolism between the cells. Without a bioavailable source of external nitrogen, 2-OG accumulates in vegetative cells (Zhang et al., 2006), and is therefore believed to serve as the signal of nitrogen insufficiency in cyanobacterial cells (Muro-Pastor et al., 2001).

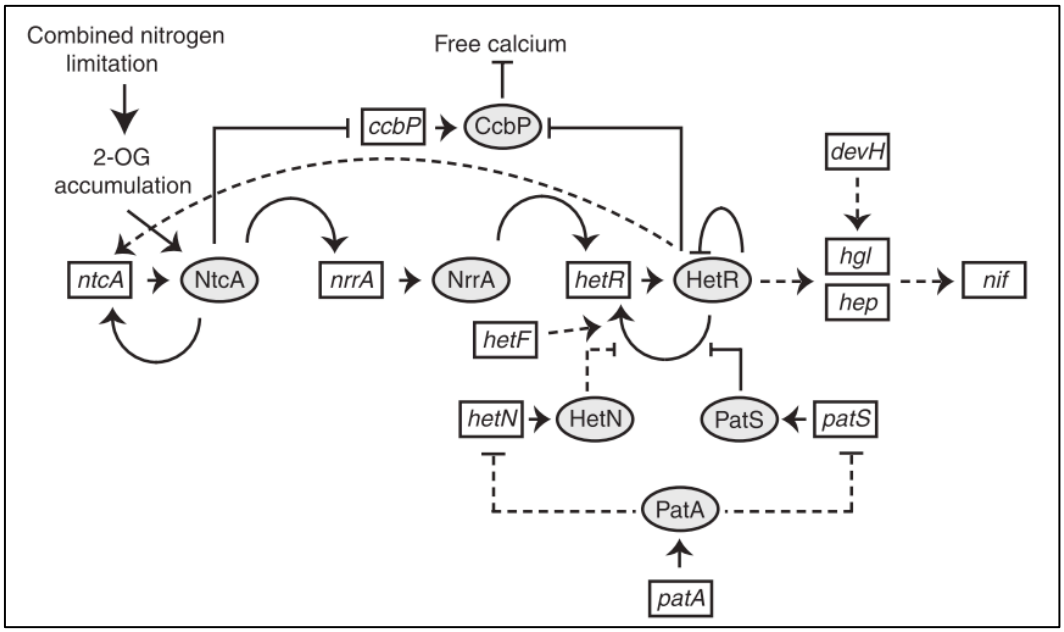

Figure 5. Schematic of important genes (boxes) and proteins (ovals) involved in heterocyst development. Positive regulation is denoted by arrows; negative regulation by flat lines. Canonical steps are indicated by solid lines; indirect or unknown interactions are represented by dashed lines. Diagram from Kumar et al. (2010).

Genes and their products: *ntcA*, *glnA*, *hetR*, *ccbP*, *patA*

On a genetic level, the increase in 2-OG may activate transcription of the *ntcA* gene whose product controls the transcription of numerous genes responsible for regulating nitrogen and carbon metabolism (Zhang et al., 2006), including *glnA*, which activates the GS-GOGAT cycle (Muro-Pastor et al., 2001). Importantly, within 3-5 hours of nitrogen starvation, the key regulatory gene *hetR* is expressed (Yoon and Golden, 2001; Torrecilla et al., 2004). The *hetR* gene product HetR either inactivates (Zhao et al., 2005) or degrades (Shi et al., 2006) the calcium-binding protein CcbP, resulting in an intracellular increase in the free Ca^{2+} ion concentration (Shi et al., 2006). This unique, heterocyst-specific calcium signal may occur before the expression of key regulatory genes involved in heterocyst development (Torrecilla et al., 2004). HetR may be sensitive to the fixed carbon to nitrogen ratio in cells, which is 4.5 under homeostatic conditions but increases to 8.1 upon depletion of fixed nitrogen reserves (Kulasooriya et al., 1972). As HetR controls the initiation of heterocyst formation (Yoon and Golden, 2001), it may lead to heterocyst differentiation above a threshold ratio of 6.1 (Buikema and Haselkorn, 1991; Kulasooriya et al., 1972). Experiments by Buikema and Haselkorn (1991) revealed the importance of *hetR* in *Anabaena* filaments, as those with nonfunctional *hetR* products fail to form any heterocysts, while *hetR* overexpression induces the formation of excess heterocysts. However, while *hetR* is required for heterocyst formation, it is not necessary for vegetative cell growth, as evident in the observation that a *hetR* disruption does not prohibit vegetative cells from forming (Buikema and Haselkorn, 1991).

Heterocyst spacing

Pattern maintenance

Given that heterocysts consume energy but do not fix carbon, and only rarely divide to yield vegetative cells that can fix carbon (Wolk, 1965), heterocysts present a substantial energy burden to the filaments. Thus, the heterocyst frequency must be tightly regulated in a spacing pattern that achieves the right balance of fixed nitrogen and carbon with minimal energy expenditure. This spacing pattern is particularly interesting in its relation to N_2 availability, which will be further discussed in chapter 4. Under modern atmospheric conditions of 0.8 bar N_2, heterocysts typically grow in a well-controlled pattern with 10-20 vegetative cells between subsequent heterocysts (Buikema and Haselkorn, 1991; Yoon and Golden, 2001) (Fig. 3). As filaments grow in length, cells divide between heterocysts until a new heterocyst is induced to develop midway between existing ones, therefore preserving the spacing pattern (Brown and Rutenberg, 2014; Thiel and Pratte, 2001).

Diffusible inhibitory signals

Several experiments (Buikema and Haselkorn, 1991; Wilcox et al., 1973; Thiel and Pratte, 2001; Yoon and Golden, 2001) have confirmed that upon formation, heterocysts control their spacing pattern by producing inhibition signals that diffuse laterally down the filament to prevent nearby vegetative cells from differentiating. This spacing is affected by growth conditions (Buikema and Haselkorn, 1991), genes and external signals (Wolk, 1989).

From a genetic basis, the product of the *patS* gene regulates heterocyst spacing along the filaments and may inhibit the ability of HetR to bind DNA (Golden and Yoon, 2003), thereby preventing heterocyst differentiation from proceeding past the initiation step. The *patS* gene encodes a pentapeptide that is expressed in differentiating cells during nitrogen starvation, playing a key role in establishing and maintaining the heterocyst pattern (Yoon and Golden, 1998; Yoon and Golden, 2001; Thiel and Pratte, 2001). Upon production, PatS is believed to diffuse laterally along the periplasmic space of filaments and inhibit neighboring cells from differentiating (Yoon and Golden, 2001). A knockout of *patS* leads to expression of adjacent heterocysts in the same cellular generation (Brown and Rutenberg, 2014), a mutation referred to as the multiple contiguous heterocyst (Mch) phenotype. In contrast, overexpression of *patS* has been correlated with excessive inhibition that blocks heterocyst development entirely (Yoon and Golden, 2001). Additionally, the *hetN* gene also leads to the production of an inhibitory ketoacyl reductase molecule HetN, which controls heterocyst spacing by suppressing adjacent cells from becoming heterocysts (Brown and Rutenberg, 2014). It is likely that HetN operates by preventing the positive autoregulation of *hetR* (Callahan and Buikema, 2001). A knockout of the *hetN* gene leads to the formation of heterocysts of different cellular generations (Brown and Rutenberg, 2014). Furthermore, the heterocyst-inducing gene *patA* is epistatic to the heterocyst-suppressing gene *patN*, which is partitioned along the side of vegetative cell membranes nearest to the septum (Risser et al., 2012). Heterocyst frequency may also be influenced by extracellular Ca^{2+} concentration and calcium agonists in *Nostoc* PCC

6720 (Smith et al., 1987; Smith and Wilkins, 1988; Zhao et al., 1991; Onek and Smith, 1992).

Fixed nitrogen

Because heterocysts form to accommodate the filaments' need for fixed nitrogen, it seems plausible that a depletion of organic nitrogen reserves below a particular threshold in vegetative cells would trigger differentiation of a new heterocyst (Kulasooriya et al., 1972). In this model, heterocyst spacing is influenced by both the rate at which fixed nitrogen propagates away from the heterocysts, and the rate of product consumption by the intervening cells. Assuming a steady consumption rate, it seems plausible that heterocyst spacing would be proportional to pN_2.

The role of fixed nitrogen as an inhibitor of heterocyst formation has also been considered (Yoon and Golden, 1998; Yoon and Golden, 2001), such that its presence may suppress the activity of molecules involved in differentiation. In this context, heterocysts may establish a proximate inhibition distance via a gradient of nitrogen fixation products that would inhibit nearby vegetative cells from differentiating into heterocysts. As the distance between heterocysts grows to a greater distance than this inhibition range, which is 12.80 ± 0.24 cells (Wolk, 1967) under current atmospheric conditions of 0.8 bar N_2, a new heterocyst could form.

Materials and Methods

Strains and culture conditions. *Anabaena cylindrica* PCC 7122 cultures were grown in the Geomicrobiology laboratories at CU Boulder in 30 ml of nitrate-containing BG-11 medium (Rippka et al., 1979) open to the atmosphere. The cells were incubated at 27°C on a 40-50 μE m^{-2} s^{-1} cool white LED panel secured to a shaking platform (100 rpm). The light panel was dimmed to the specific illumination using a voltage regulating microcontroller, and the cultures were enclosed to eliminate external lighting. The BG-11 media was supplemented with 20 mM HEPES to buffer pH (pKa 7.5) and the media pH was adjusted to 7.8 with NaOH.

All *Anabaena variabilis* experiments were conducted at the Microbial Ecology/ Biogeochemistry Research Laboratory at the NASA Ames Research Center. *A. variabilis* ATCC 29413 cultures were grown in 200 ml of non-supplemented nitrate-containing BG-11 medium open to the atmosphere in a 22°C incubator with a 12h:12h light:dark cycle; lights on at 0700 h. Filaments were exposed to 30 μE m^{-2} s^{-1} without shaking during growth.

Heterocyst pattern. To induce heterocyst formation in *A. variabilis*, heterocyst-free filaments were collected by centrifugation, then triple washed with and resuspended in 8-10 ml of $BG\text{-}11_0$ media lacking nitrate. Resuspended filaments were sealed in septum bottles and exposed to variable pN_2 at total headspace pressure of 1 bar (balance He), which was mixed in Tedlar gas sampling bags (Zefon International, Inc, Ocala, FL). Experiments were run for either 4 or 10 days without replenishing the headspaces. Culture growth was measured daily by optical density at 750 nm wavelength through the culture bottles (i.e. without sample withdrawal) using a

DR2700 portable spectrophotometer (Hach, Loveland, CO), and final headspace composition was measured with a Shimadzu 14A gas chromatograph (Shimadzu, Kyoto, Japan). N_2 was separated from O_2 on a molecular sieve packed column, using helium as the carrier gas, and analyzed by a thermal conductivity detector. Matheson Tri-gas 20% O_2/79%N_2 was run as a standard along with the samples. Four biological replicates of samples were prepared for each pN_2 tested. Suspension experiments were run for 4 days, then cell cultures were immediately fixed with 4% paraformaldehyde and refrigerated at 4°C. For microscopy, samples were carefully pipetted onto glass slides to avoid breaking filaments.

A. cylindrica cultures were inoculated with 1% washed week-old cultures grown in BG-11 medium at atmospheric CO_2 and were nitrogen limited throughout the growth experiments. The headspace of the anaerobic culture tubes was a mixture of 0.2 bar CO_2, variable pN_2, and a He balance (1 bar total), generated in a gas mixing cylinder via a custom-built gas blending station using three thermal mass flow controllers calibrated for CO_2, N_2 and He, respectively. Growth experiments were run for either 15 days without replenishing the headspace, or for 11 days with replenishing the headspace on the 7^{th} day. For each nitrogen condition, four biological replicates and one abiotic control were included. Culture growth was measured daily by optical density at 750 nm wavelength through the culture tube using a Spectronic 20D+ spectrophotometer. Cultures were harvested after stationary phase by fixation with 3% paraformaldehyde and subsequently stored in the refrigerator at 8°C. When headspace was not replenished regularly, final headspace composition of cultures was confirmed using a Model 8610C gas chromatograph (SRI Instruments, Torrance, CA) fitted with a 2

m long, 2 mm ID SilcoSmooth tubing packed with ShinCarbon ST 80/100 mesh stationary phase (Restek part number 80486-800, Bellefonte, PA) and a thermal conductivity detector.

In the *A. cylindrica* culture growth timing experiments, headspaces were replenished daily beginning at early-exponential growth phase (OD_{750} = 0.1 to 0.2). 200 µl samples were withdrawn from each condition at early–exponential (t = 5 d), late–exponential (t = 8 d) and death (t = 16 d) phases of culture growth, then fixed with 3% paraformaldehyde and refrigerated at 8°C until microscopic examination.

Microscopy. For *A. variabilis* experiments, bright-field microscopy was used to identify heterocysts visually. Micrographs were taken on a Nikon Microphot-FXA microscope (Nikon, Tokyo, Japan), and images were captured with a Carl Zeiss AxioCam HRc camera (Carl Zeiss AG, Oberkochen, Germany). For *A. cylindrica* experiments, heterocysts were determined visually by bright-field microscopy coupled with autofluorescence (Mariscal et al., 2007) achieved through illumination by a halogen lamp and propidium iodide filter cube. Micrographs were taken on a Zeiss Axio Imager.Z1 (Carl Zeiss Microscopy, Peabody, MA) with a 40x air objective, and images were captured with a Zeiss AxioCam MRm camera (Carl Zeiss Microscopy, Peabody, MA).

In addition to standard methods for visual identification of heterocysts (Yoon and Golden, 2001), lack of autofluorescence was used as an indicator for heterocyst identification in *A. cylindrica* filaments. Protoheterocysts were counted as mature heterocysts, and intervals were quantified by the number of vegetative cells scored between successive heterocysts. Cells were considered whole if a distinct septum

separated two adjacent cells. The observation of numerous detached heterocysts indicated a possible underestimation of average interval length. Taking filament breakage into consideration, the terminal vegetative cell sequences were recorded for estimates of the minimum distance between adjacent heterocysts. All intervals on each given filament were measured, and successive intervals from the same filament were noted for future analyses of correlation. Over 250 heterocyst intervals were counted for each condition. Interval lengths are reported as the number of vegetative cells between successive heterocysts. No akinetes were observed in any samples.

Statistical analyses. Given the large number of heterocyst intervals counted for each pN_2 condition, statistical significance was computed using a Student's t test in spite of the non-Gaussian distribution of heterocyst spacing at each pN_2. For a regression analysis of heterocyst distance vs. pN_2, a one-tailed two-sample t test with a 95% confidence interval was used to assess whether the mean heterocyst distance of filaments cultivated under lower pN_2 was significantly less than that of filaments cultivated under a higher pN_2 for all possible pairwise combinations of mean heterocyst distances at pN_2 = 0, 0.1, 0.3, 0.5 and 0.8 bar in both *A. variabilis* and *A. cylindrica* studies. A two-tailed t test was used to determine whether significant variation existed between mean heterocyst distances within and between experiments, including between filaments grown under the same pN_2 across different experiments. Only p values < .05 were considered statistically significant. Data are reported as the mean and median heterocyst distance (# cells) ± 1σ.

Results

Heterocyst spacing in *Anabaena cylindrica* in response to pN_2

Anabaena cylindrica PCC 7122 cultures were cultivated under different nitrogen partial pressures (pN_2 = 0, 0.1, 0.3, 0.5, 0.8 bar) immediately following nitrate deprivation to examine whether atmospheric pN_2 levels influence heterocyst spacing. Four biological replicates and one abiotic control (BG-11_0 medium without cells) were included for each nitrogen condition. For cultures induced under $pN_2 > 0$ bar, heterocysts were easily distinguishable from the brighter vegetative cells because they showed reduced autofluorescence due to their lack of light-harvesting phycobiliprotein. A compilation of bright-field and fluorescence micrographs of heterocystous filaments grown under each pN_2 condition is provided in Figure 6, and highlights the average increase in heterocyst distance observed at each subsequently higher pN_2. Filaments cultivated at pN_2 = 0 bar developed heterocysts at closely spaced intervals but exhibited inconsistent and occasionally reversed patterns of autofluorescence that were not useful for heterocyst identification. These cultures did not show significant growth (as measured by optical density) and likely succumbed to nitrogen starvation so vegetative cells were unable to maintain phycobiliprotein and actively photosynthesize. Proheterocysts were counted as heterocysts in consideration that they would ultimately terminally differentiate.

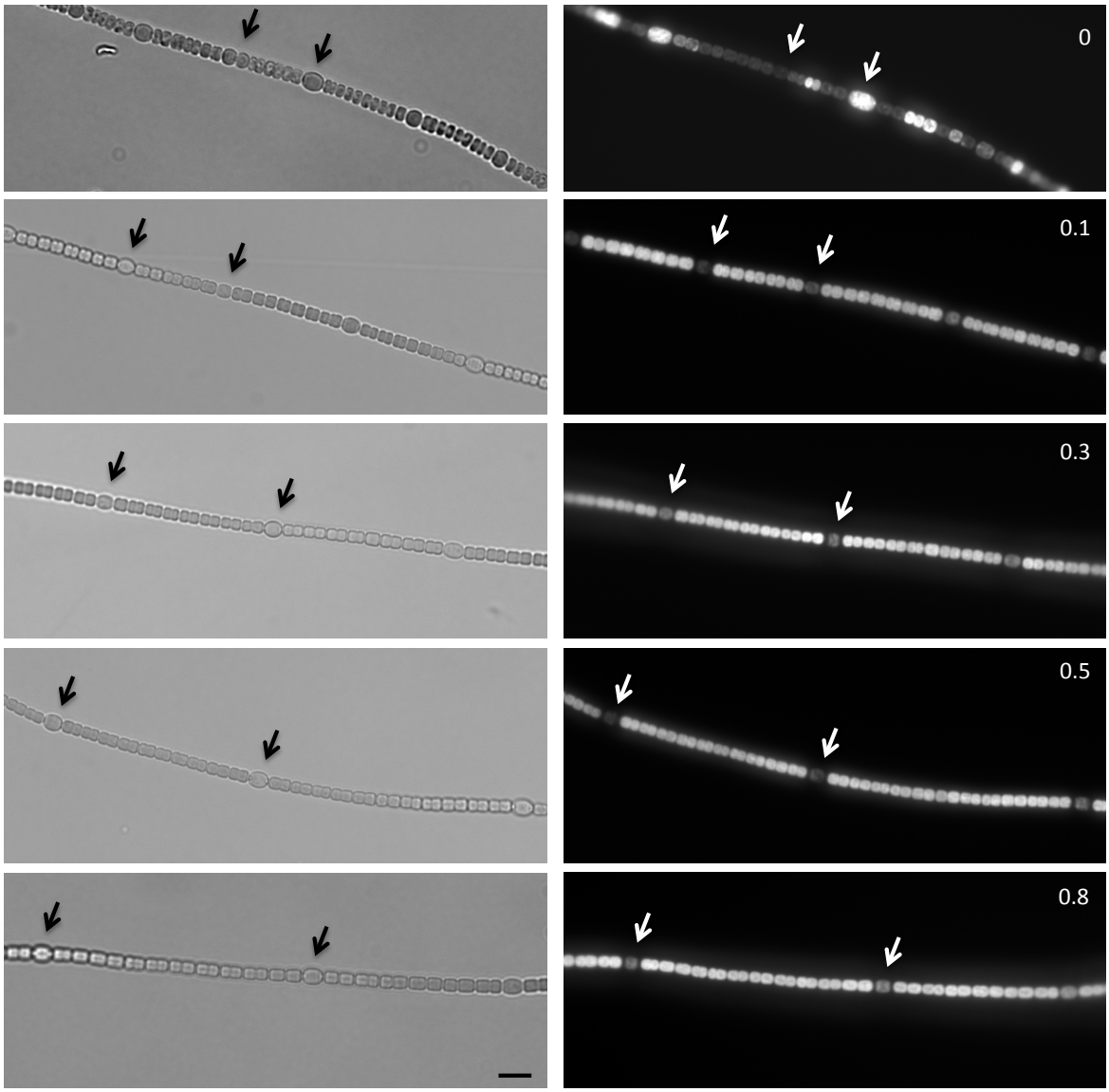

Figure 6. In descending order: *Anabaena cylindrica* PCC 7122 filaments grown in nitrogen-free BG-11_0 media for 11 days under pN_2 = 0, 0.1, 0.3, 0.5 and 0.8 bar respectively. Corresponding micrographs were taken in bright-field (left panels) and fluorescence (right panels). Mean distance between heterocysts (denoted by arrows for one representative interval) increased in filaments cultivated at higher pN_2. Scale bar, 10 μm.

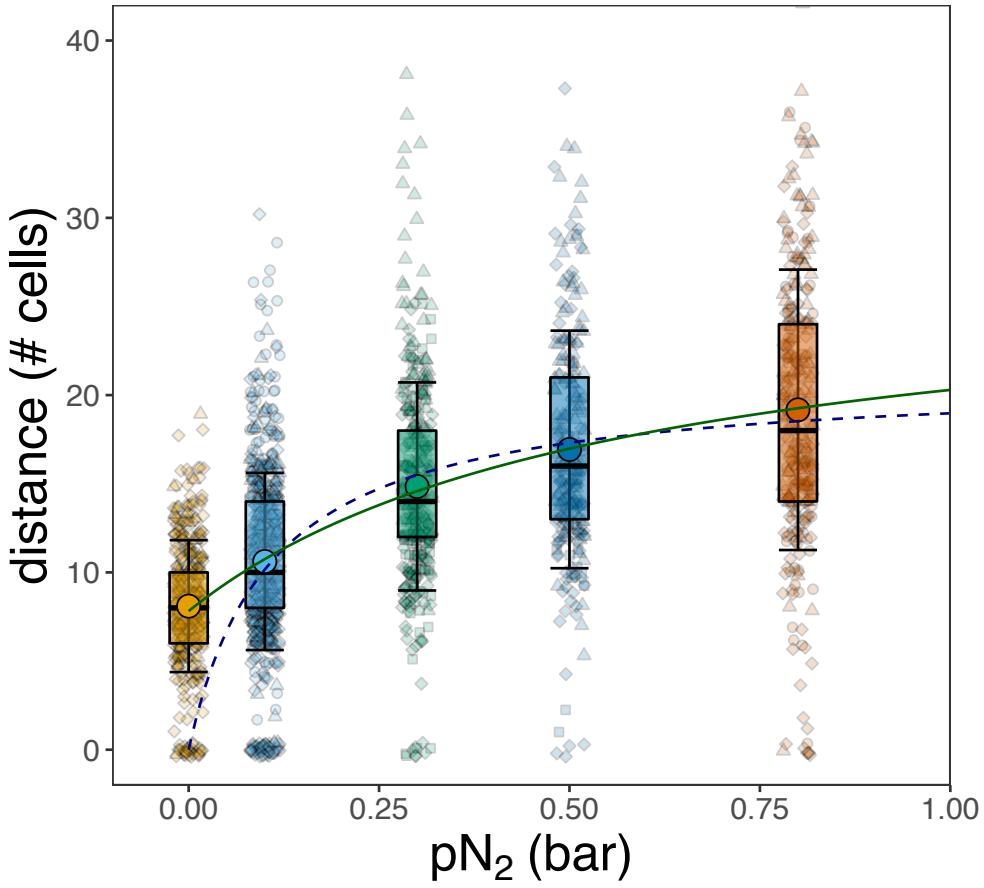

Figure 7. *Anabaena cylindrica* PCC 7122 heterocyst distances in response to pN_2. *A. cylindrica* grown in liquid BG-11 medium were induced to develop heterocysts in nitrogen-free BG-11_0 under variable N_2 partial pressures. Cells were harvested after stationary phase of culture growth. Over 250 vegetative cell sequences between consecutive heterocysts were counted for each pN_2 condition. Each sequence is represented by one data point on the plot; symbols distinguish the experiments conducted. Distribution of heterocyst distances for each pN_2 is presented as a box plot showing the mean (circle), median (center line), interquartile range (box height) and error bars of ±1σ. A nonlinear least squares fit following the Michaelis-Menten model of enzyme kinetics (Eq. 3) was plotted with (dashed blue; K_M = 0.11 ± 0.013 bar N_2) and without (solid green) a forced calibration through zero.

Table 1. *Anabaena cylindrica* PCC 7122 heterocyst distances in response to N_2 partial pressure.

$\mathbf{pN_2}$ *(bar)*	$\bar{x}_{\mathbf{het}}$ *(# cells)*	$\mathbf{M_{het}}$ *(# cells)*	$\mathbf{1\sigma}$ *(# cells)*
0	8.0	8	3.6
0.1	10.2	10	4.9
0.3	12.1	12	5.5
0.5	13.7	13	5.9
0.8	15.6	15	7.5

Summary of the data represented in Figure 7. Measurements of heterocyst distance for each pN_2 are reported as: mean ($\bar{x}_{het}$), median (M_{het}) and one standard deviation (1σ). A one-tailed two-sample t test revealed that for all pairwise comparisons, heterocyst distances were significantly shorter in filaments cultivated at lower N_2 partial pressures than at high ($p < .001$ for all significant combinations).

The number of vegetative cells between heterocysts was used to quantify separation distances and an average was computed for each pN_2 condition. Results are reported as the mean and median heterocyst distance with one standard deviation in units of cells (Table 1). At each subsequently higher pN_2 tested, the average heterocyst distance increased by ~2 cells within the range of 8 to 15 cells. Analysis of the results by a one-tailed two-sample t test between any pair of N_2 partial pressure conditions revealed that the mean heterocyst distance in all filaments exposed to the lower pN_2 was significantly less than the mean of those exposed to the higher pN_2 ($p < .001$ in all pairwise comparisons).

Overall, heterocyst spacing appeared to increase as a hyperbolic function of pN_2, reflecting saturation of nitrogenase with increasing N_2 during nitrogen fixation. Using the Michaelis-Menten model of enzyme kinetics (Eq. 3) and the assumption that heterocyst differentiation is triggered by a low threshold of nitrogen availability in individual vegetative cells, the following relationship was derived:

$$\text{heterocyst distance} = c\,V_{\max}\,\frac{[pN_2]}{K_M + [pN_2]} \quad (2)$$

where c is an arbitrary constant. Heterocyst distances were plotted against $\frac{[pN_2]}{K_M + [pN_2]}$ in a linear model with slope $c\,V_{\max}$, and residual analysis using the means of the data from 0.1 to 0.8 bar N_2 yielded an optimum K_M value of 0.11 ± 0.013 bar N_2 for nitrogen fixation (Fig. S3). Data from pN_2 = 0 bar were excluded from this calculation, as these cultures likely lacked nitrogen fixation activity. A curve generated from our model $c\,V_{\max}\,\frac{[pN_2]}{K_M + [pN_2]}$ with K_M = 0.11 ± 0.013 bar N_2 was fitted to our data (Fig. 7, dashed blue line). A second best-fit curve including data from pN_2 = 0 bar was determined through the same approach, but the K_M value yielded from this model did not accurately reflect nitrogen fixation rates, and so was not reported here.

It was interesting to note the occurrence of adjacent heterocysts (Fig. 8; indicated as a vegetative cell interval of 0 in Fig. 7) under all pN_2 conditions, but a greater proportion was observed in the two lowest pN_2 conditions. Due to their potential physiological significance, both heterocysts in a contiguous pair were included in the cell counts. It is possible that this led to an overrepresentation of heterocysts, as proheterocysts (young heterocysts) are known to sometimes initially form in pairs from newly divided sibling cells that compete for nutrients until only one terminally differentiates (Buikema and Haselkorn, 1991; Meeks and Elhai, 2002). In some species heterocysts always form in pairs (Komárek and Anagnostidis, 1989; Gordon and Gordon, 2016). However, when the average distance was computed excluding

contiguous heterocysts, the mean heterocyst distance did not change by more than one cell count (Table S1).

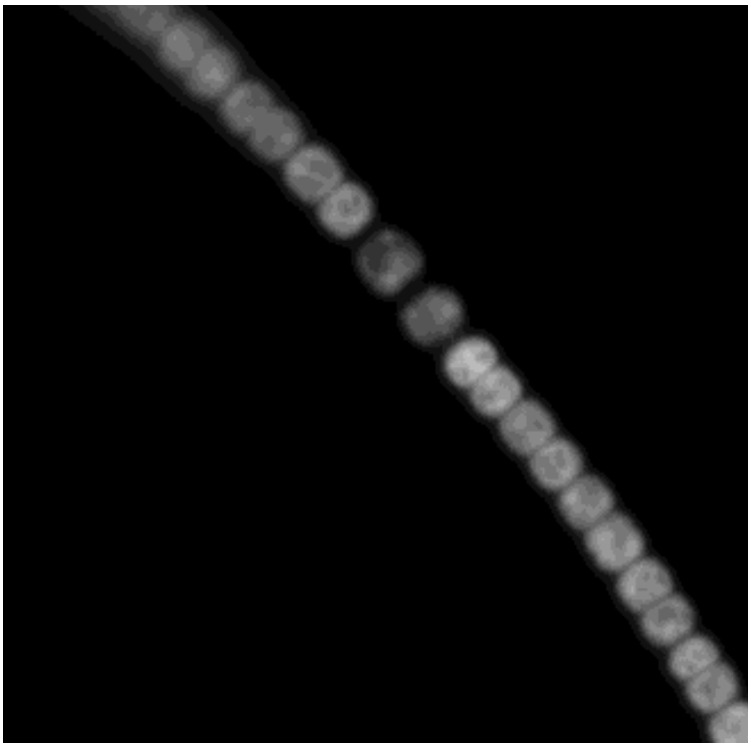

Figure 8. Pair of contiguous heterocysts (dark) in *Anabaena cylindrica* PCC 7122 filament cultivated under 0.1 bar N_2 for 16 days. This phenotype was observed in cultures grown under all pN_2 conditions, but most frequently arose at pN_2 = 0 and 0.1 bar.

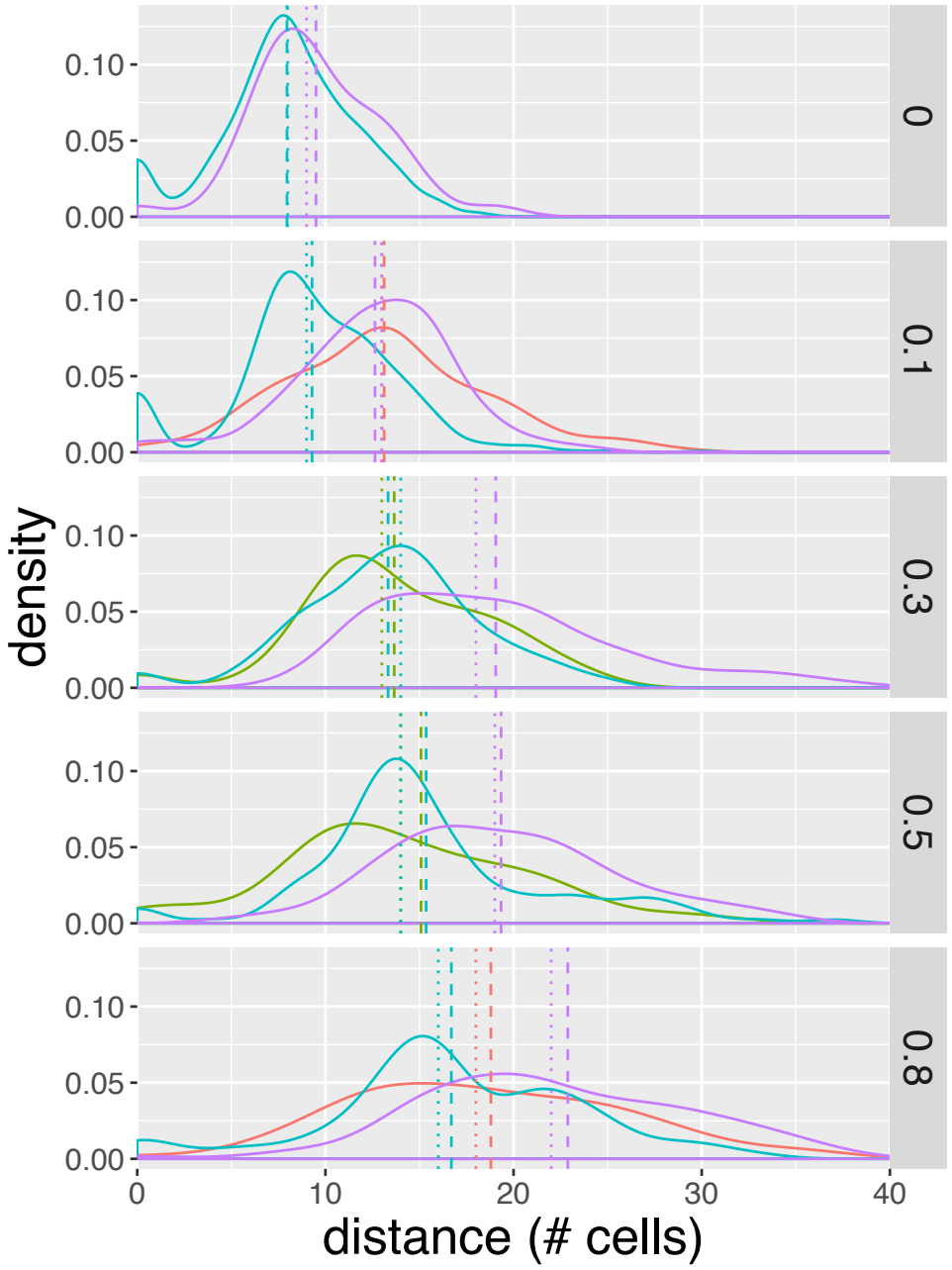

Figure 9. Distribution of heterocyst spacing (from Fig. 7) for *Anabaena cylindrica* strain PCC 7122 across multiple experiments. Results are grouped by pN_2 for comparison; in descending order: pN_2 = 0, 0.1, 0.3, 0.5 and 0.8 bar. Each of the 4 experiments compared is depicted by color in chronological order of experiment performed: red, green, blue, purple. The mean (dashed lines) and median (dotted lines) heterocyst distances increased with pN_2, but showed substantial biological variation across experiments.

The quantifiable influence of pN_2 on heterocyst spacing was complicated by the large variation in spacing that occurred between individual filaments and across cultures grown under the same pN_2 in separate experiments (Fig. 9). In order to examine whether the heterocyst pattern fluctuates over time, which may explain this variation, samples were extracted at three phases of culture growth: early–exponential (t=5 d), late–exponential (t=8 d) and death (t=16 d) during the course of the experiment (Fig. 10A), and heterocyst distances were recorded (Table 2). At t=5 d, cultures growing in absence of N_2 did not develop enough biomass to be extracted and consequently could not be included in the cell counts. Overall, the absolute heterocyst distance was not preserved as filaments grew, but rather the relative spacing of heterocysts in each condition was maintained over time and increased with higher pN_2 levels (Fig. 10B).

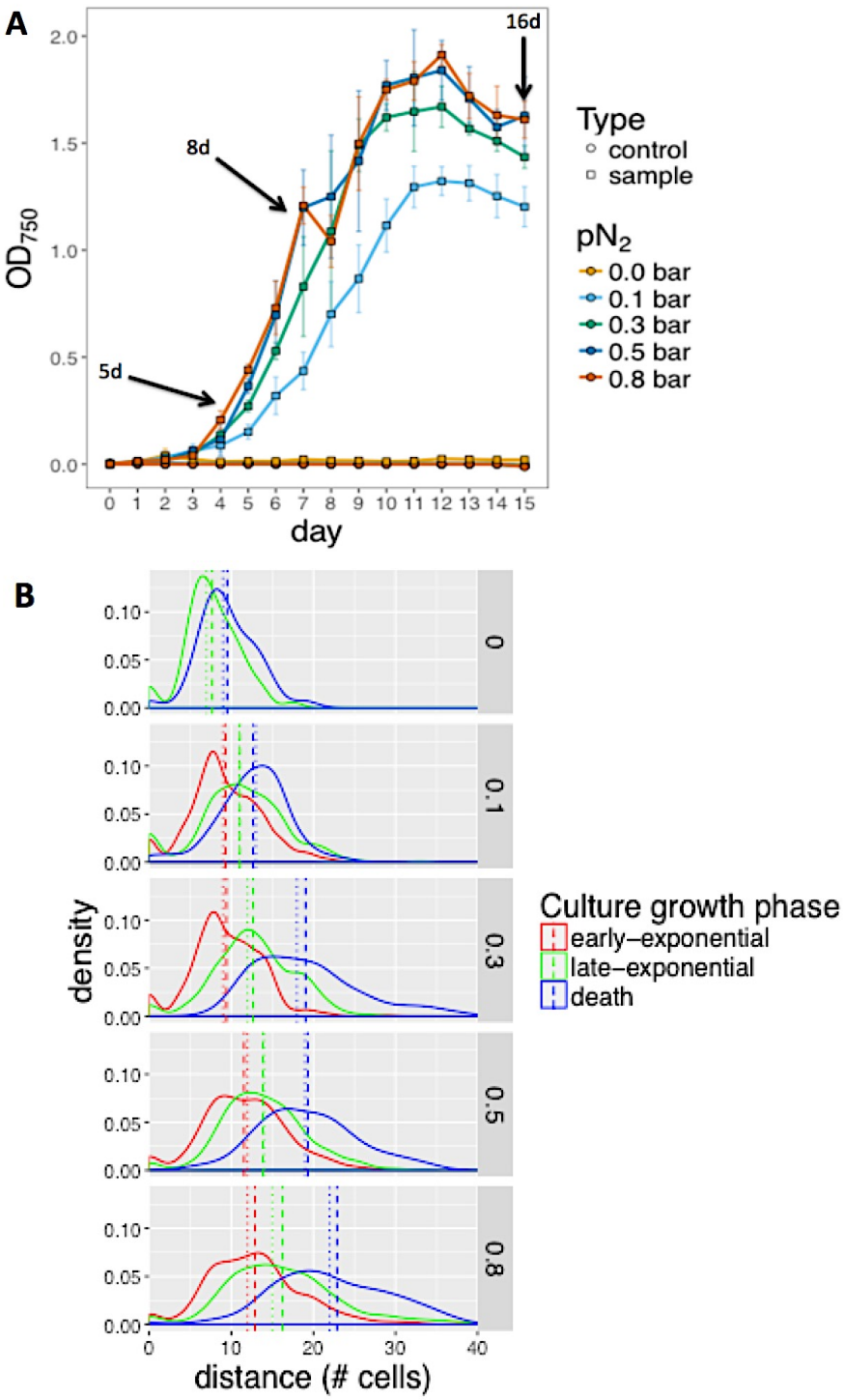

Figure 10. Heterocyst culture growth timing experiments for *Anabaena cylindrica* PCC 7122. *A. cylindrica* cultures were induced to develop heterocysts in nitrogen-free BG-11_0 media under different N_2 partial pressures. (A) Samples were harvested at t = 5 d, 8 d and 16 d, and heterocyst distances were recorded. (B) In descending order of panels: pN_2 = 0, 0.1, 0.3, 0.5 and 0.8 bar. Within each N_2 conditions, the mean (dashed lines) and median (dotted lines) heterocyst distances increased over the three culture growth phases examined.

Table 2. *Anabaena cylindrica* PCC 7122 heterocyst distances over time in response to N_2 partial pressure.

	5 d		8 d		16 d	
pN_2 *(bar)*	**$\bar{x}_{het}$** *(# cells)*	**1σ** *(# cells)*	**$\bar{x}_{het}$** *(# cells)*	**1σ** *(# cells)*	**$\bar{x}_{het}$** *(# cells)*	**1σ** *(# cells)*
0	–	–	7.70	3.35	9.50	3.47
0.1	9.33	4.52	11.07	5.48	12.63	4.25
0.3	9.42	4.24	12.70	4.94	19.05	6.45
0.5	11.56	5.16	13.87	5.16	19.34	5.96
0.8	12.87	6.01	16.27	7.37	22.88	8.03

Summary of the data represented in Figure 10. Measurements of heterocyst distance for each pN_2 are reported as: mean ($\bar{x}_{het}$), median (M_{het}) and one standard deviation (1σ).

Given that longer filaments are statistically more susceptible to breakage and that heterocyst death often leads to breakage at the heterocyst-vegetative cell interface (Herrero et al., 2004), it is possible that the mean heterocyst distance computed for each nitrogen condition was lower than the actual value. Taking this into consideration, vegetative cell sequences between terminal heterocysts and the ends of the filaments were recorded, and lower bounds for possible unrecorded interval lengths were calculated for every sample. All terminal sequences fell within heterocyst-bound interval lengths previously recorded, precluding the need for further investigation.

Furthermore, filaments cultivated under $pN_2 \leq 0.1$ bar aggregated into biofilms on the glass surfaces of the tubes, presumably either as a survival mechanism in response to the substantial nitrogen limitation (Garrett et al., 2008), or as a result of the mucilage secreted by the filaments to propagate their gliding movements (Walsby, 1967). Though analysis of this phenomenon was beyond the scope of this project, future

bacterial adhesion studies could provide interesting insight into the physiological and genetic mechanisms mediating this response.

Heterocyst spacing in *Anabaena variabilis* in response to pN_2

Anabaena variabilis cultures were initially grown without nitrogen limitation and subsequently washed and suspended under different nitrogen partial pressures (pN_2 = 0, 0.1, 0.3, 0.5, 0.8, 1 bar) in nitrogen-limiting conditions. The heterocyst pattern in *A. variabilis* filaments did not appear to respond to nitrogen levels (Fig. 11). Analysis of the results by a one-tailed two-sample t test revealed that overall, the mean heterocyst distances did not follow the pattern observed in *A. cylindrica*. However, it was acknowledged that the amount of data collected for this species was substantially less than that of the *A. cylindrica* experiments, so future experiments may be required to confirm these results.

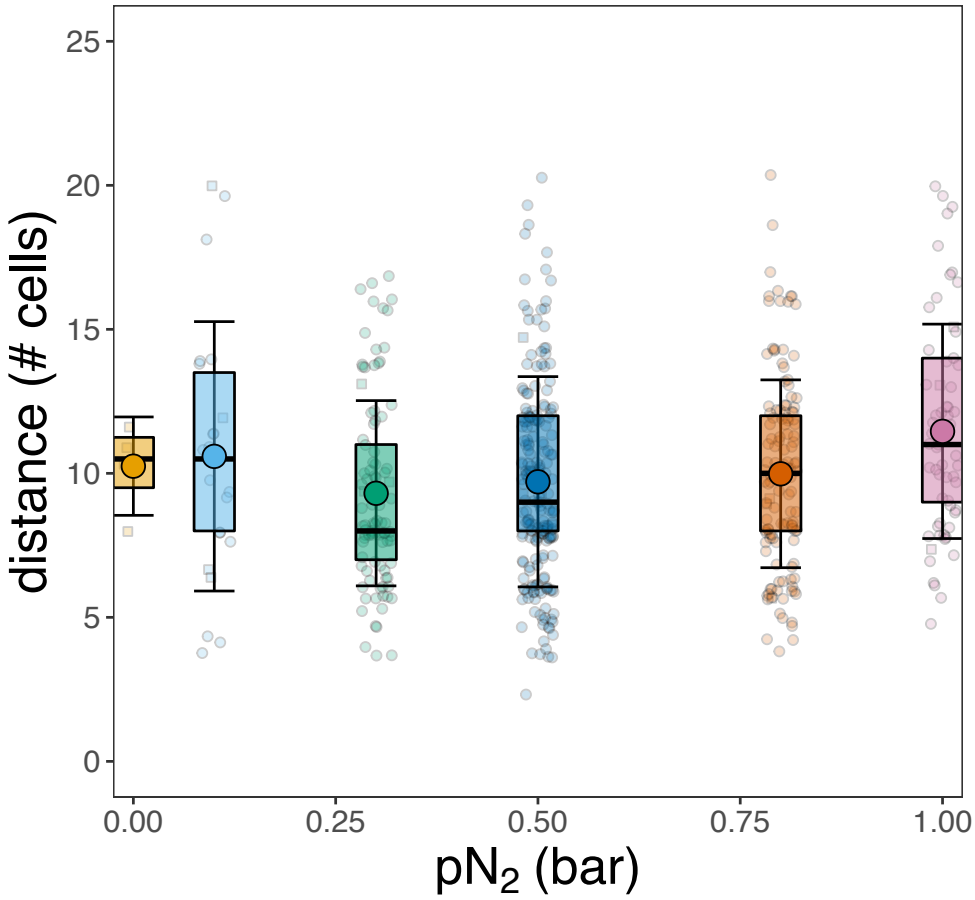

Figure 11. *Anabaena variabilis* ATCC 29413 heterocyst distances in response to pN_2. *A. variabilis* grown in liquid BG-11 medium were induced to develop heterocysts in nitrogen-free BG-11_0 under variable N_2 partial pressures. Cells were harvested after 4 or 10 days. Approximately 75 vegetative cell sequences between consecutive heterocysts were counted for each pN_2 condition. Each sequence is represented by one data point on the plot; symbols distinguish the two different experiments conducted. Distribution of heterocyst distances for each pN_2 is presented as a box plot showing the mean (circle), median (center line), interquartile range (box height) and error bars of ±1σ , which were not symmetric about the median. Overall, heterocyst distance did not appear to correlate to pN_2.

Table 3. *Anabaena variabilis* ATCC 29413 heterocyst distances in response to N_2 partial pressure.

$\mathbf{pN_2}$ *(bar)*	$\bar{x}_{\mathbf{het}}$ *(# cells)*	$\mathbf{M_{het}}$ *(# cells)*	$\mathbf{1\sigma}$ *(# cells)*
0	10.2	10.5	1.7
0.1	10.6	10.5	4.7
0.3	9.3	8	3.2
0.5	9.7	9	3.7
0.8	9.9	10	3.3
1	11.5	11	3.7

Summary of the data represented in Figure 11. Measurements of heterocyst distance for each pN_2 are reported as: mean ($\bar{x}_{het}$), median (M_{het}) and one standard deviation (1σ). A one-tailed t test revealed that for all pairwise comparisons, heterocyst distance did not significantly vary, except between those cultivated under pN_2 = 1 bar and pN_2 = 0.3 bar ($p < .001$), 0.5 bar ($p < .001$), 0.8 bar ($p < .01$). Overall, heterocyst spacing did not appear to correlate to pN_2.

Discussion

Anabaena cylindrica

Our findings support our hypothesis that heterocyst spacing is regulated by pN_2 in *Anabaena cylindrica*. Overall, the average distance between intercalary heterocysts showed a hyperbolic increase with pN_2 (Fig. 7), highlighting the possible role of enzyme kinetics as a rate-limiting factor in interval lengthening. Here I offer a model for how the heterocyst pattern may be regulated by pN_2, with the assumption that nitrogen fixation rates solely depend on nitrogenase, and that the overall spacing is a linear reflection of these rates due to one-dimensional diffusion of and differentiation triggered by fixed nitrogen along the filament. With these assumptions, heterocyst spacing could be used as a proxy for enzyme kinetics without directly quantifying the V_{max} of nitrogenase. The Michaelis-Menten equation for rates of enzymatic reactions is given by the following (Cornish-Bowden, 1979):

$$v_o = V_{max} \frac{[S]}{K_M + [S]} \quad (3)$$

where v_o and V_{max} describe the observed and maximum reaction rates respectively, $[S]$ refers to the substrate concentration (here, the dissolved concentration of aqueous N_2), and K_M is the substrate concentration at $\frac{1}{2}V_{max}$. Incorporating this equation into our model of heterocyst spacing control by nitrogen fixation (Eq. 2), we created nonlinear fits that included data at 0 bar N_2 (Fig. 7, solid green curve) and excluded this data with a forced calibration through zero (Fig. 7, dashed blue curve), respectively. The zero intercept curve yielded a half-saturation constant K_M of 0.11 ± 0.013 bar N_2 for nitrogen fixation. This half-saturation constant was similar to a previously reported value of 0.2 for *A. cylindrica* (Ohmori and Hattori, 1972), which was directly estimated through

acetylene-reduction assays. A nonlinear fit using K_M = 0.2 bar N_2 was superimposed on our previous curve of K_M = 0.11 ± 0.013 bar N_2 for visual comparison (Fig. S4). Given that our K_M value was not assessed through the direct measurement of nitrogenase activity, it appears that heterocyst distance can serve as a good proxy for nitrogen fixation rates. Diffusional limitations, if present, would otherwise preclude a direct relationship between N_2-fixation and N_2 diffusion rates, but were not accounted for in our calculations.

Further support for our model, while acknowledging these limitations, is the fact that the concentration of dissolved aqueous N_2 available for nitrogen fixation is directly proportional to the pN_2 above the liquid by Henry's law:

$$H^{cp} = c_a / p \quad (4)$$

where H^{cp} (the constant for Henry's law solubility) for N_2 gas in water is 6.0 x 10^{-4} mol L^{-1} bar^{-1} (Sander, 2015), c_a is the aqueous concentration of N_2 (M), and p is the partial pressure of N_2 at equilibrium (bar). The dissolved N_2 gas does not easily cross the three-membrane envelope of heterocysts, so instead it must be taken up by vegetative cells and transported into heterocysts through connecting terminal pores (Walsby, 2007). From observations on gas-vesicle collapse in *Anabaena flos-aquae* (Walsby, 1985), the rate of gas diffusion into a heterocyst is given by:

$$dC/dt = \alpha(C_o - C_i) \quad (5)$$

where dC/dt is the rate of change in gas concentration inside the heterocyst (M s^{-1}), α is the exponential filling rate of the heterocyst (s^{-1}), C_o is the gas concentration outside the heterocyst (M) and C_i is the concentration inside (M) (Walsby, 2007). Assuming that the amount of N_2 diffusing into the vegetative cells is directly proportional to the amount of

N_2 available in the aqueous phase ($C_o \cong c_a$), Eq. 4 and Eq. 5 can be combined to derive a new equation relating the rate of gas diffusion into a heterocyst to the partial pressure of the gas:

$$dC/dt \cong \alpha(p * H^{cp} - C_i) \quad (6)$$

Given that the N_2 concentration difference ($C_o - C_i$, Eq. 5) determines the rate at which N_2 enters heterocysts, it can be inferred that a higher pN_2 (and thus aqueous N_2) would increase the rate of N_2 diffusion into the heterocysts. At equilibrium, the rate of N_2 diffusion into the heterocyst must equal the N_2-fixation rate (Walsby, 2007); however, taking enzyme kinetics into consideration, nitrogen fixation rates will asymptotically approach V_{max} as nitrogenase becomes saturated with N_2 and is unable to keep up with N_2 entry into the heterocyts. Thus, the rates of nitrogen fixation (Eq. 3) and N_2 gas diffusion into a heterocyst (Eq. 6) can be related by the final equation:

$$\frac{V_{max}[S]}{K_M + [S]} \propto \alpha(p * H^{cp} - C_i) \quad (7)$$

Flores et al. (2006) suggest that the periplasm serves as a channel through which substances can be exchanged between heterocysts and vegetative cells. Given that this transport is most likely mediated by passive diffusion, the rate at which fixed nitrogen propagates away from the heterocysts should be proportional to the rate of fixation. Assuming a steady consumption rate of nitrogen, the distance a pool of organic nitrogen can emanate before being completely metabolized by intervening vegetative cells will depend on its diffusional rate. The vegetative cells midway between existing heterocysts would consequently become starved for nitrogen as filaments lengthen. At some point, the organic nitrogen concentration must cross a low threshold, thereby

triggering heterocyst formation (Yoon and Golden, 1998; Yoon and Golden, 2001). This threshold may be encoded as an intracellular ratio of fixed carbon to nitrogen that rises above 6.1 (Kulasooriya et al., 1972), and is sensed by the master regulator HetR (Buikema and Haselkorn, 1991).

To summarize our proposed model, the distance at which a new heterocyst will form relative to a parent heterocyst should scale linearly with the rate of fixed nitrogen supplied by the parent heterocyst. Enzyme kinetics underlying the overall growth kinetics would cause heterocyst spacing to correlate hyperbolically with pN_2. While this model is first order, it is consistent with the observed heterocyst pattern. I acknowledge that reducing heterocyst spacing to nitrogenase activity alone may be oversimplifying the mechanisms occurring, and that nitrogen fixation rates may not be solely dependent on N_2 partial pressure. For example, in nature, bacteria are known to enhance nitrogenase activity of *Anabaena* species by consuming O_2 near the heterocysts, while cyanobacteria excrete products that enrich bacterial growth (Paerl, 1978). The axenic cultures used in this study lacked such a symbiotic relationship, so it is possible that the nitrogen fixation rates operating here do not accurately represent those observed in natural cyanobacterial communities. However, a model that takes into consideration all possible environmental and biological effects on heterocyst spacing is beyond the scope of this thesis.

The importance of unaccounted factors was highlighted by the significant variation in spacing observed between individual filaments and across cultures grown under the same pN_2 in separate experiments (Fig. 9). Gas chromatography measurements revealed that for the cultures in which the headspace was not

replenished, the cells had consumed a significant amount of CO_2 by the end of each experiment. It is possible that a lack of carbon for carbon fixation inhibited mechanisms that normally regulate the heterocyst pattern thereby masking their natural response to pN_2. Additionally, heterocyst differentiation may be influenced by cell cycle timing (Yoon and Golden, 2001; Meeks and Elhai, 2002), so it is possible that the variation observed was a consequence of the point at which, in their cell cycles, the filaments were harvested. Though this phenomenon was not investigated at the individual cellular level here, our culture growth timing experiments highlighted the possible macro-influence of culture growth phase on heterocyst differentiation. Within each pN_2 condition, the average heterocyst distance appeared to increase as the cultures progressed through the early–exponential, late–exponential and death phases (Fig. 10), potentially as a consequence of the increasing energy and nutrient deprivation. In contrast to the energetically inexpensive growth and division of vegetative cells, heterocyst differentiation requires substantial energy and nutrients. The exponential phase of culture growth is characterized by rapid cell division, which likely includes rapid heterocyst differentiation. It is possible that during this phase, shorter heterocyst intervals were maintained because the abundance of media nutrients enabled heterocyst differentiation to keep up with vegetative cell division. Upon nutrient depletion (late–exponential phase), the rate of vegetative cell division may have surpassed differentiation of heterocysts, manifested in the overall lengthening of heterocyst intervals. Heterocyst differentiation may have completely halted in the death phase, but resilient vegetative cells continuing to divide with residually available fixed nitrogen would have furthered filament lengthening. Additionally, vegetative cells may

have consumed fixed nitrogen at higher rates during the early stages of culture growth, which could have also led to the shorter intervals observed. Regardless, these phenomena would not have been specific to pN_2, and therefore were observed across all pN_2 conditions.

In addition to our proposed model for pN_2 influence on differentiation, it is possible that the concentration of N_2 is perceived by sensing systems that genetically regulate heterocyst spacing in cyanobacteria. Given that organic nitrogen availability is encoded in 2-OG levels (Muro-Pastor et al., 2001) perceived by NtcA, a global transcriptional activator of heterocyst differentiation (Herrero et al., 2004), the buildup of 2-OG in response to combined nitrogen deprivation may scale with aqueous N_2 concentration. In the same manner, higher N_2 concentrations may either cause the downregulation of heterocyst-activating genes such as *hetR* (Buikema and Haselkorn, 1991), or the upregulation of heterocyst-inhibiting genes such as *pastS*, *hetN* or *patN*, which encode diffusible molecules that inhibit differentiation of cells nearby to heterocysts (Yoon and Golden, 2001; Thiel and Pratte, 2001; Callahan and Buikema, 2001; Risser et al., 2012). Calcium levels are also known to influence heterocyst spacing (Torrecilla et al., 2004; Shi et al., 2006) and therefore may be regulated by N_2 levels. For calcium in particular, future studies capitalizing on the calcium-triggered luminescence of the photoprotein aequorin (Knight et al., 1991; Torrecilla et al., 2004) could provide interesting insight into whether such a relationship exists.

The occurrence of adjacent heterocysts in filaments cultivated under the lower pN_2 conditions was not surprising, but the reason for their development at higher N_2 levels was unclear. This multiple contiguous heterocyst (Mch) phenotype has been

observed in mutant strains of heterocystous cyanobacteria that either lack key inhibitory genes such as *patS* that regulate the heterocyst pattern (Brown and Rutenberg, 2014), or that overexpress genes that promote heterocyst formation, such as *hetR* (Buikema and Haselkorn, 1991). It is known that some vegetative cells adjacent to heterocysts show transient differences in fluorescence properties (Cardona et al., 2008), so it is possible that some nonheterocystous cells were included in the cell counts. However, the majority of heterocysts were distinguished by their physical characteristics in addition to their lack of fluorescence, so a miscounting of this sort would not have contributed significant error to the data.

Overall, the heterocyst pattern in *A. cylindrica* appears to correlate with pN_2 levels, but the extent to which this is regulated, and the direct mechanisms underlying this response merit further investigation.

Anabaena variabilis

The apparent absence of a response to pN_2 in *Anabaena variabilis* may reflect the different mechanisms that contribute to the heterocyst pattern in the two species investigated here. Most *Anabaena* organisms contain a Mo-dependent nitrogenase expressed by the *nif1* gene cluster (Brusca et al., 1989; Herrero and Wolk, 1986). This nitrogenase is expressed exclusively in heterocysts under oxic conditions (Elhai and Wolk, 1990; Thiel et al., 1995). In *A. variabilis,* a second Mo-nitrogenase can be expressed by the *nif2* gene cluster under anoxic conditions in all vegetative cells (Schrautemeier et al., 1995; Thiel et al., 1997; Thiel et al., 1995). Although either nitrogenase can independently satisfy the nitrogen requirements of the filaments, they

can be expressed simultaneously (Thiel et al., 1997). It is likely that the functional redundancy of nitrogenase expression in *A. variabilis* precluded the ability of pN_2 to influence heterocyst spacing. Whereas our nitrogen gradient model can explain some of the trend observed in *A. cylindrica*, it does not seem probable that a similar gradient would exist in *A. variabilis* because the Nif2 nitrogenases, located in the vegetative cells, can provide enough fixed nitrogen to satisfy their own cell's needs. It is instead likely that the Nif2 nitrogenase was expressed first under the initial anoxic conditions, but the buildup of molecular oxygen produced by the photosynthetic vegetative cells induced expression of the Nif1 nitrogenase and formation of heterocysts.

In attempt to explain the fact that heterocysts can still differentiate in *nif1* mutant strains of *A. variabilis* that express fully functional Nif2 nitrogenases, Thiel and Pratte (2001) proposed the idea that heterocyst development is not controlled by the nitrogen insufficiency of individual cells, but rather is a uniform response to nitrogen deprivation in the external environment. However, given our findings in the *A. cylindrica* experiments, it is more likely that intracellular sensing mechanisms do trigger differentiation upon nitrogen starvation, but that the Nif2 nitrogenase in *A. variabilis* produces enough fixed nitrogen throughout the filaments that a regulated heterocyst pattern does not occur. Perhaps the Nif1 and Nif2 nitrogenases are redundantly expressed when the *A. variabilis* filaments perceive an external nitrogen deficiency in order to increase their chances of survival (Thiel and Pratte, 2001).

It is also possible that different signals trigger heterocysts to differentiate in the two species, which would render the comparison between heterocyst differentiation mechanisms difficult. Additionally and perhaps most noteworthy, CO_2 was not included

in the headspaces of the *A. variabilis* cultures, which would have induced severe carbon limitation in these experiments. If heterocyst differentiation is indeed triggered by an increase in the fixed C:N ratio above a threshold, a low concentration of fixed carbon could prevent heterocyst differentiation of nitrogen-starved cells, which would essentially outweigh the cells' need for fixed nitrogen. It has been previously demonstrated that the transfer of cyanobacterial cells from high to low CO_2 conditions (5% to 0.035% in air, respectively) induces global metabolic reprogramming that yields concomitant signals of nitrogen starvation and nitrogen sufficiency (Eisenhut et al., 2008). In the *A. variabilis* experiments, this would have undoubtedly affected the heterocyst spacing pattern. Thus, if the heterocyst spacing pattern in *A. variabilis* filaments does indeed respond to pN_2, it is possible that experimental artefacts from carbon limitation prevented such a pattern from being observed.

The differences in response to pN_2 by *A. variabilis* and *A. cylindrica* could not be reconciled in this study and merit future research.

Conclusions

In this portion of my thesis, I examined whether two species of cyanobacteria, *Anabaena variabilis* and *Anabaena cylindrica*, can record information about atmospheric N_2 levels in the heterocyst spacing pattern of their filaments. Our hypothesis that increased N_2 partial pressure (pN_2) would lead a greater number of vegetative cells to form between heterocysts along the one-dimensional filaments was derived from the following assumptions: (i) intracellular nitrogen starvation of vegetative cells triggers heterocyst differentiation; (ii) fixed nitrogen is transported along the filaments via passive diffusion; (iii) vegetative cells consume fixed nitrogen at a uniform rate; coupled with the following known parameters: (i) the concentration of dissolved aqueous N_2 is directly proportional to pN_2 by Henry's law; (ii) an increased $[N_2]$ induces a faster rate of nitrogen fixation by nitrogenase until saturation, by Michaelis-Menten enzyme saturation kinetics. In order to test this, I cultivated heterocyst-free filaments in nitrate-free media under variable pN_2 and recorded the number of vegetative cells between adjacent heterocysts to quantify separation distances. Due to possible carbon limitation, redundant nitrogenase expression or various other unknown reasons, the heterocyst spacing pattern in *A. variabilis* filaments did not appear to respond to pN_2. In contrast, *A. cylindrica* filaments showed a hyperbolic increase in heterocyst spacing with pN_2, which not only supported our hypothesis, but also highlighted the fact that heterocyst distance is mediated by enzyme kinetics. Such a response has not previously been shown, and further examination of this effect may improve our current understanding of the mechanisms that lead to heterocyst differentiation and pattern maintenance in these cyanobacterial species. Though our findings offer potential in this

aspect, the large biological variability in heterocyst spacing at each pN_2 condition, coupled with the fact that this response may be species-specific, prevents this morphological phenomenon from likely becoming a useful geobarometer. This conclusion will be discussed in detail in chapter 4.

CHAPTER THREE

Nitrogen Isotopic Fractionation by *Anabaena cylindrica* PCC 7122 is Influenced by N_2 Partial Pressure

Abstract

Biological nitrogen fixation contributes the main flux of fixed nitrogen to the global nitrogen cycle. As accumulated biomass moves through the biogeochemical cycles, isotope effects imposed by enzymes lead to a potentially distinct and measurable isotopic signature. In particular, fractionation ($\delta^{15}N$) of newly fixed nitrogen by Mo-nitrogenase is $-1 \pm 1‰$, which highlights its preference for ^{14}N, the lighter nitrogen isotope. These measurements have been reported for nitrogenase operating under the nitrogen replete conditions of the present atmosphere (0.79 bar N_2), but the effect of N_2 availability on overall cellular isotope fractionation has not been explored in nitrogen fixation. Here I show that Mo-nitrogenase in *Anabaena cylindrica* PCC 7122 produces fixed nitrogen with more positive $\delta^{15}N$ values (i.e. weaker fractionation) under N_2 limited conditions, which suggests that its inherent isotope discrimination is compromised during substrate deficiency.

Introduction

Like other light elements of major biological importance, nitrogen has a minor naturally occurring stable isotope (^{15}N) of one mass unit heavier than its most abundant form, ^{14}N. Despite the fact that the isotopes have similar properties and can participate in the same chemical reactions, they may exhibit different reaction rates due to their varying reaction kinetics and bond energies (Schoeller, 1999; Zhang et al., 2014). Lighter isotopes usually have slightly faster reaction rates in enzymatic processes and therefore tend to be preferentially incorporated in biosynthetic assimilation reactions such as carbon and nitrogen fixation, producing isotopically light biomass. The exact degree of discrimination against heavy isotopes is influenced by an enzyme's intrinsic isotope effect (ε_{fix}), and is specific to individual enzymes and reactions. These isotope effects are physical processes that may result in isotope fractionation, or partial separation of isotopes, which can be observed in participating reactants and products (Hayes, 2004). As biogeochemical cycles progress through time, fractionation patterns can change in response to major shifts in the relative importance of key biogeochemical processes, and will differ between material generated by reactions that exhibit different isotopic preferences. Because isotope ratios typically vary at and beyond the third significant figure, it is not useful to report them as fractional abundances. Instead, natural isotopic variations are typically discussed in the context of their relative change in ratio of heavy to light isotope of a sample compared to that of a designated isotopic standard. Expression of these relative isotope abundances are often reported in conventional delta notation (δ), expressed in permil (‰, parts per thousand) as follows:

$$\delta = \left[\frac{R_{\text{sample}}}{R_{\text{standard}}} - 1\right] \times 1000 \quad (8)$$

where R is the ratio of the heavy to light isotope. For nitrogen, $\delta^{15}N$ denotes the fractionation of biomass relative to standard atmospheric N_2 (defined as 0‰). In contrast, $\varepsilon^{15}N_{Norg/N2}$ (‰) represents the difference between fractionation of nitrogen isotopes in the biomass produced by nitrogenase relative to that of the nitrogen source, atmospheric N_2 ($\delta^{15}N_{Norg} - \delta^{15}N_{N2}$). Because both $\delta^{15}N$ and $\varepsilon^{15}N$ are referenced against atmospheric N_2 in the case of nitrogen fixation, $\delta^{15}N = \varepsilon^{15}N$.

For nitrogen flux through the cells, the nitrogen isotope ratio is not significantly altered as atmospheric N_2 diffuses into vegetative cells, along the periplasmic space of the filaments and into heterocysts. The most substantial fractionation occurs during nitrogen fixation and is induced by the isotope effect of nitrogenase (Fig. 12), which has been directly estimated to be –17‰ for the purified enzyme (Sra et al., 2004). In contrast, the average organism-wide $\delta^{15}N$ of newly fixed nitrogen by Mo-nitrogenase has been measured as –1 ± 1‰ (Zhang et al., 2014). It has been hypothesized that the reduced discrimination against ^{15}N in cellular-contained nitrogenase may be a consequence of limited N_2 availability (Unkovich, 2013). Such a proposition has not yet been tested, but if true, N_2 availability could be recorded within the nitrogen isotope composition of the filaments. In turn, the isotopic composition of the filaments could be used as a proxy for atmospheric nitrogen levels, which will be further assessed in chapter 4.

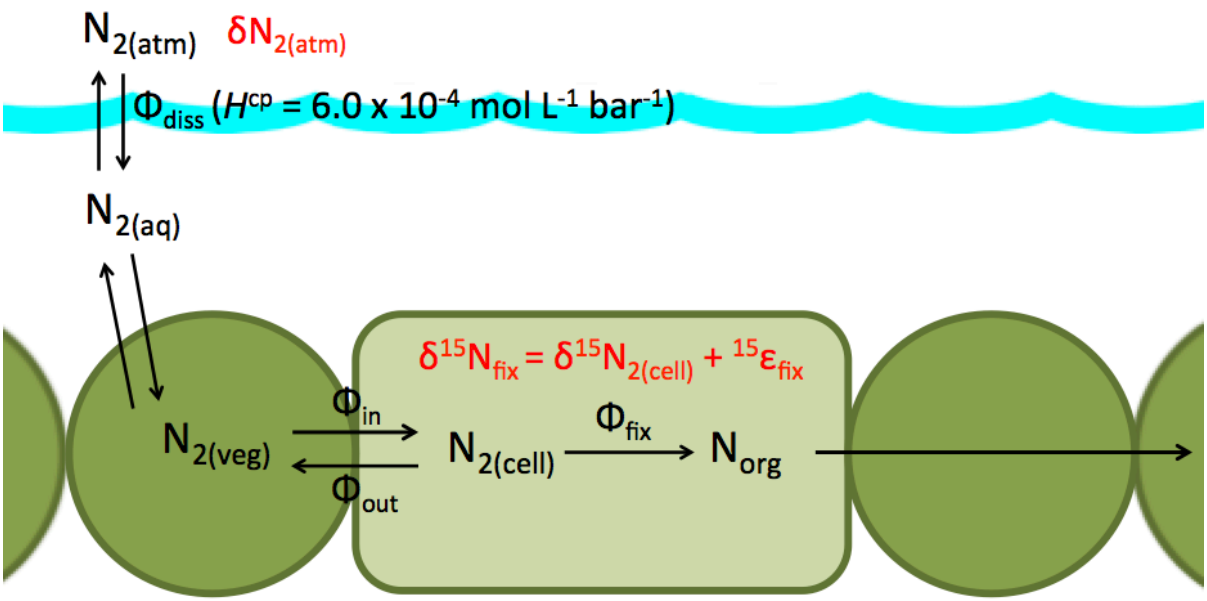

Figure 12. Steady state flux model of nitrogen movement through a cyanobacteria filament. The concentration of N_2 gas that dissolves in the aqueous phase is proportional to the pN_2 above the liquid; H^{cp} is Henry's law solubility constant for N_2 gas in water (Sander, 2015). N_2 diffuses into the vegetative cells (round) and through the heterocyst (rectangular) to be fixed. The isotope effect ($^{15}\varepsilon_{fix}$) imposed by nitrogenase during nitrogen fixation causes the most significant fractionation of isotopes ($\delta^{15}N_{fix}$) relative to atmospheric N_2 ($\delta N_{2(atm)}$) in this pathway.

Materials and Methods

Strains and culture conditions. At the end of the heterocyst culture growth timing experiments, all remaining *Anabaena cylindrica* PCC 7122 cells that had not been harvested for heterocyst spacing measurements were collected for isotope analysis. For detailed information on culture conditions, see chapter 2 "Materials and Methods".

Nitrogen isotope analysis. Samples for isotope analyses were collected by vacuum filtration onto 0.8 μm glass-fiber filters pre-combusted at 500°C, following methods used in Zhang et al. (2014). Approximately 750 μg of dry biomass were combusted in tin capsules by an elemental analyzer (Flash 2000) coupled to an isotope ratio mass spectrometer (Thermo Delta V Plus). All sample preparation and analysis was carried out at the CU Boulder Earth Systems Stable Isotope Lab (CUBES-SIL). Isotope abundances of the samples were reported as $\delta^{15}N_{Norg/N2}$ (‰) and plotted as $\varepsilon^{15}N_{Norg/N2}$ (‰) in reference to the standard and the source for nitrogen fixation (both atmospheric N_2), respectively. The calculation performed for $\delta^{15}N$ followed Eq. 8, which is directly defined for nitrogen here as:

$$\delta^{15}N_{Norg/N2} = \left[\frac{R_{Norg}}{R_{N_2}} - 1\right] \times 1000 \quad (9)$$

where R is the ratio of $^{15}N/^{14}N$. Similarly, $\varepsilon^{15}N_{Norg/N2}$ (‰) is defined here as $\delta^{15}N_{Norg} - \delta^{15}N_{N2}$. Because $\delta^{15}N$ and $\varepsilon^{15}N$ are both referenced against atmospheric N_2, $\varepsilon^{15}N_{Norg/N2} = \delta^{15}N_{Norg/N2}$ in this case.

The raw nitrogen isotopic measurements were calibrated against two acetanilide laboratory standards with known $\delta^{15}N$ values of +1.18 ± 0.02‰ and +19.56 ± 0.03‰. All data was linearity, blank and offset corrected based on these two isotopic

standards across a nitrogen signal range of 2.2 μmol (300 μg) to 5.9 μmol (800 μg). The biomasses of all the samples were within this range.

Statistical analyses. Results of $\varepsilon^{15}N_{Norg/N2}$ are reported as the mean ± 1σ (in ‰). Significance of the effect of pN_2 on the isotope effect of nitrogenase was determined through a simple linear regression model.

Results

To evaluate whether the pN_2 is reflected in the isotopic signature of nitrogen fixation by nitrogenase in *A. cylindrica*, samples from the previous heterocyst culture growth experiments were collected, and the $\delta^{15}N_{biomass}$ of each culture was determined. Fractionation of biomass from each pN_2 condition are reported in Table 3 as the mean and standard deviation (in ‰) of four biological replicates per condition. At pN_2 = 0 bar, the cultures did not yield enough biomass to be collected for isotope analysis, and thus were not included in the results. Here, I report net isotopic effects $\varepsilon^{15}N_{Norg/N2}$ between biomass nitrogen and atmospheric nitrogen (assumed to be 0‰). It is important to note that the actual net biological effect is likely slightly smaller due to equilibrium fractionation of N_2 between the gaseous and dissolved phases. Previous studies have shown that dissolved aqueous N_2 has a higher abundance of ^{15}N, yielding an isotopic enrichment of 0.1 – 0.6‰ relative to atmospheric N_2 (Benson and Parker, 1961; Emerson et al., 1991).

Our $\delta^{15}N$ of biomass produced under 0.8 bar N_2 fell within the range (0.5 to –2.8‰) of previously measured $\delta^{15}N$ values for diazotrophic cyanobacteria grown under current atmospheric conditions of 0.79 bar N_2 (Zhang et al., 2014; Bauersachs et al., 2009). Globally, nitrogen fixation is believed to introduce organic matter with a $\delta^{15}N$ of approximately –1 ± 1‰, as inferred from measurements of newly fixed nitrogen by Mo-nitrogenases (Minagawa and Wada, 1986; Carpenter et al., 1997). The $\delta^{15}N$ of *A. cylindrica* in particular, growing under atmospheric N_2 levels, has been measured as –1.6‰ (Bauersachs et al., 2009). Thus, the $\delta^{15}N$ of our cultures cultivated under 0.8 bar N_2 (–2.5‰,) aligned with those of previous studies.

The numerical fractionation of fixed nitrogen relative to the atmospheric pool ($\varepsilon^{15}N_{Norg/N2}$) showed a strong, inverse relationship with pN_2 (Fig. 13, $r^2 = 0.86$), indicating that a higher proportion of ^{14}N was fixed under increased N_2 availability. From the steady state flux model of nitrogen movement through the cells (Fig. 12), the following equation can be derived:

$$\varepsilon^{15}N_{Norg/N2} = \left(1 - \frac{\Phi_{fix}}{\Phi_{in}}\right) * \varepsilon_{fix} \quad (10)$$

Taking enzyme kinetics into consideration (Eq. 3), it can be hypothesized that:

$$\frac{\Phi_{fix}}{\Phi_{in}} \propto \frac{\frac{[pN_2]}{K_M+[pN_2]}}{[pN_2]} = \frac{1}{K_M+[pN_2]} \quad (11)$$

giving the final proportionality equation:

$$\varepsilon^{15}N_{Norg/N2} \propto \frac{1}{K_M+[pN_2]} \quad (12)$$

$\varepsilon^{15}N_{Norg/N2}$ was plotted against $\frac{1}{K_M+[pN_2]}$ in a simple linear regression using our previously estimated K_M of 0.11 ± 0.013 bar N_2, and the results showed a hyperbolic correlation between $\varepsilon^{15}N$ and $\frac{\Phi_{fix}}{\Phi_{in}}$ (Fig. 14).

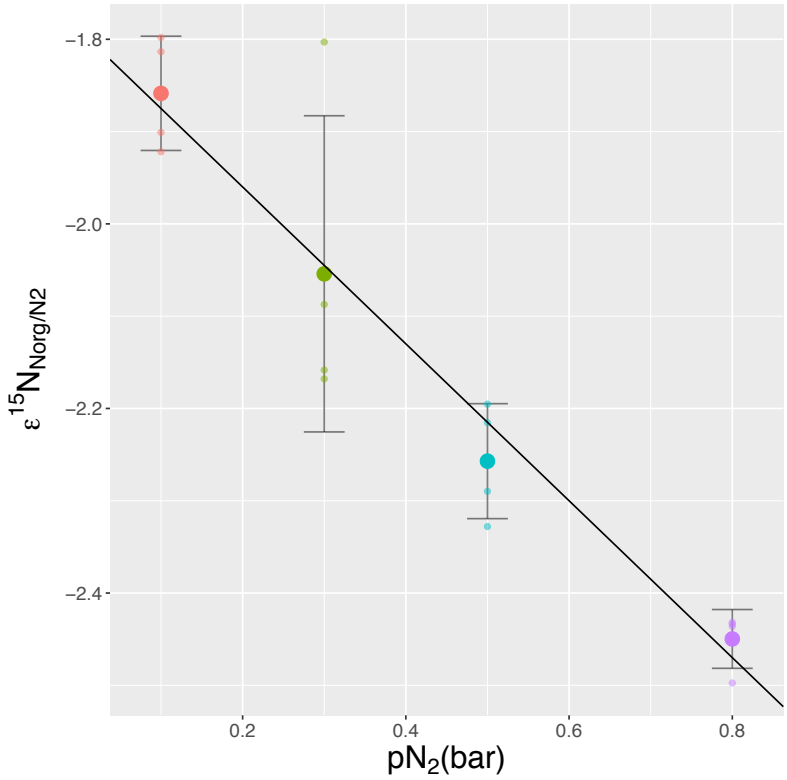

Figure 13. $\varepsilon^{15}N_{Norg/N2}$ (‰) of biomass from *Anabaena cylindrica* PCC 7122 cultivated under different N_2 partial pressures. *A. cylindrica* organisms were grown under different pN_2 conditions for 16 days in the heterocyst growth phase experiments. All samples remaining that had not been collected for heterocyst spacing analysis were collected and analyzed for nitrogen isotopic fractionation. Cultures grown under pN_2 = 0 bar did not yield enough biomass and had to be omitted from isotope analysis. $\varepsilon^{15}N_{Norg/N2}$ of biomass from 4 biological replicates per pN_2 showed a clear correlation with pN_2 (r^2 = 0.86).

Table 3. $\delta^{15}N$ (in ‰ vs. air N_2) of biomass from *Anabaena cylindrica* PCC 7122 cultivated under different N_2 partial pressures.

pN_2 *(bar)*	**$\delta^{15}N_{Norg/N2}$** (‰)	**1σ** (‰)
0.1	-1.86	0.06
0.3	-2.05	0.17
0.5	-2.26	0.06
0.8	-2.45	0.03

Quantitative values for the data represented in Figure 13, summarized here as the mean $\delta^{15}N_{Norg/N2}$ and one standard deviation (‰) from four biological replicates of each pN_2 condition. Overall, the numerical fractionation decreased linearly with pN_2.

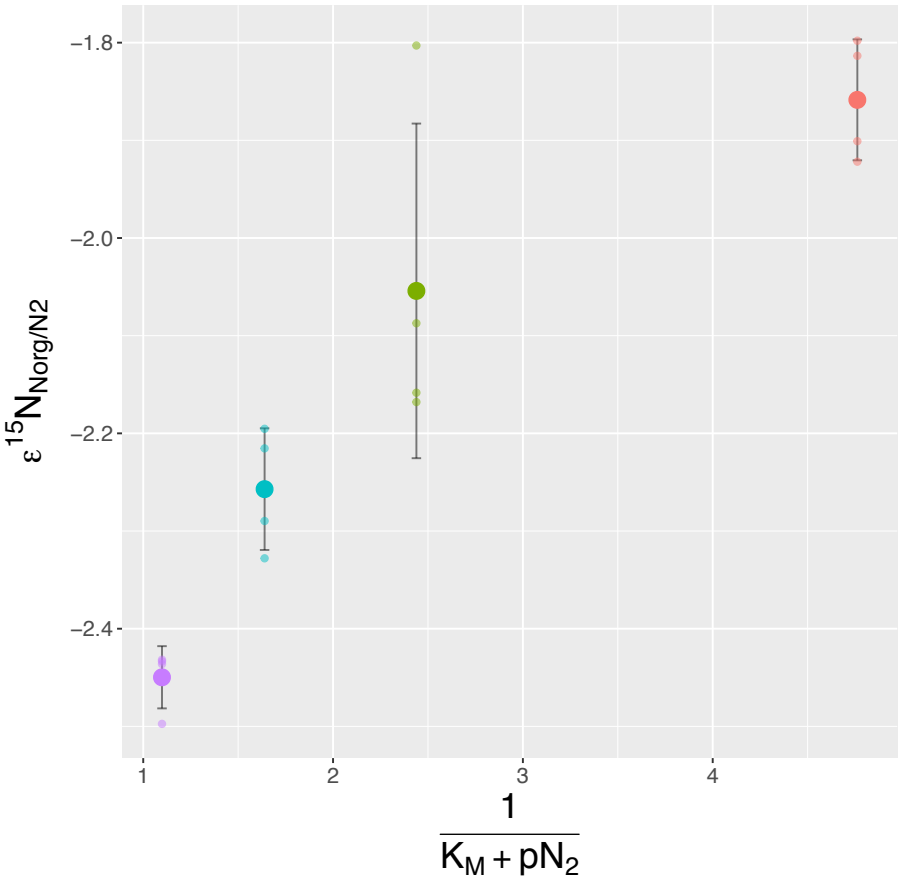

Figure 14. $\varepsilon^{15}N_{Norg/N2}$ (‰) of biomass from *Anabaena cylindrica* PCC 7122 from Table 3, plotted against the proportion of nitrogen fixed from the total influx $\left(\frac{\Phi_{fix}}{\Phi_{in}}\right)$, where $\Phi_{fix} \propto v_o$ (the rate of nitrogen fixation given by Eq. 3), and $\Phi_{in} \propto pN_2$. A more complete derivation of $\frac{1}{K_M + [pN_2]}$ can be found in Eqs. 10-12. Results showed a hyperbolic correlation.

Discussion

The strong correlation between isotopic fractionation ($\varepsilon^{15}N_{Norg/N2}$) of fixed nitrogen and pN_2 in the *Anabaena cylindrica* filaments suggests that the tendency for nitrogenase to discriminate against the heavier nitrogen isotope (^{15}N) during nitrogen fixation is compromised under conditions of low N_2 availability. In nature, reactions tend to favor the lighter isotopes because the bonds of these molecules can be broken with less energy. As such, nitrogenase displays an intrinsic isotope effect (ε_{fix}) during nitrogen fixation, generating biomass with a specific fractionation of nitrogen isotopes that can be maintained as long as the pool of atmospheric nitrogen in heterocysts is continually exchanged with the extracellular world. I believe that this scenario occurs at higher pN_2, because flux of N_2 into the vegetative cells and down the filaments would be faster overall. However, here I see different isotopic signature of fixation at each pN_2, suggestive of the fact that lower N_2 availability reduces the exchange rate of the cellular N_2 pool with the atmosphere, and thus with every ^{14}N molecule that nitrogenase incorporates during fixation, the remaining cellular N_2 pool becomes subsequently enriched in ^{15}N. This enriched nitrogen isotopic composition of residual dissolved N_2 in the heterocysts consequently leads nitrogenase to fix N_2 with a greater proportion of ^{15}N than that derived from the original N_2 pool regardless of its intrinsic isotope fractionation. This is reflected in the weaker overall fractionation of nitrogen isotopes observed in filament biomass at a lower pN_2.

It is also possible that a greater abundance of heterocysts could contribute to a higher $\varepsilon^{15}N_{Norg/N2}$. Proteins and chlorophylls have been found to be depleted in ^{15}N by about 1.2‰ relative to the cell as a whole (Chikaraishi et al., 2005), so the reduced

abundance of chlorophyll in cultures grown under low pN_2 may have contributed to the isotopic ratio observed. Contribution to this fractionation by alternative nitrogenases, which are known to cause a pronounced effect (Zhang et al., 2014) can be ruled out, as *A. cylindrica* only possesses a single Mo-nitrogenase (Attridge and Rowell, 1997). Given the clear influence of pN_2 on the isotopic composition of organic nitrogen produced by nitrogenase, it may be possible to quantify the currently unknown intrinsic ε_{fix} of Mo-nitrogenase in *A. cylindrica* in future studies.

Conclusions

In this portion of my thesis, I examined whether a limited availability of N_2 changes the extent to which nitrogenase's inherent isotope discrimination is expressed. Such an effect has been previously proposed (Unkovich, 2013), and has been demonstrated in other isotopic systems (i.e. sulfate reduction), but has not been experimentally explored in nitrogen fixation. Given the role of enzyme kinetics in the distinct isotope fractionation patterns of biomass produced by alternative nitrogenases (Zhang et al., 2014), I hypothesized that low N_2 partial pressure, and thus limited N_2 availability, would affect the kinetics of nitrogenase and thereby modulate its isotopic signature. Fractionation of biomass from *Anabaena cylindrica* PCC 7122 cultures appeared to scale with pN_2 such that biomass at high pN_2 was isotopically enriched in the lighter isotope. Low N_2 availability appeared to compromise the isotope effect of nitrogenase, leading to a weaker fractionation observed in these cultures. Overall, these findings supported my hypothesis and further suggest that N_2 availability can be recorded in the nitrogen isotope composition of the filaments. As such, if biomass from heterocystous nitrogen fixing bacteria is preserved in the rock record, this information will be a key asset to understanding past nitrogen cycles.

CHAPTER FOUR

Applications to Paleoatmospheric Constraints: the Potential for New Geobarometers

The rigorous search for new ways to study the paleoatmosphere is driven by a variety of motivations, including to better understand Earth's ancient environmental conditions, reconcile the 'faint young Sun paradox', and assess whether extrasolar planets may be habitable based on their atmospheric constituents. However, studying ancient atmospheres is difficult because physical properties of atmospheres, such as density and pressure, have minimal impacts on rocks. Numerous methods (Som et al., 2012; Som et al., 2016; Marty et al., 2013; Berner, 2006) have helped constrain both total air pressure and the partial pressures of individual gases at specific timepoints in Earth's history (Fig. 1), but it is clear that our understanding of the paleoatmosphere is heavily data-limited, thus warranting the search for new geobarometers that can help to further constrain our current estimates.

Cyanobacteria are ancient organisms that continue to thrive today. As such, current species can be used as proxies for ancestral strains, enabling us to potentially extrapolate information about the environment during their life. The question of when cyanobacteria first evolved is one that is heavily disputed. Conservative analyses constrain their evolution to ~2.35 billion years (Ga) ago (Kopp et al., 2005; Ward et al., 2015), but evidence of fossilized cyanobacteria in stromatolites indicates their existence 2.5 – 2.8 Ga ago (Schopf and Walter, 1982; Buick, 2008). Still, other claims point to the possibility of their evolution a billion years prior to these records (Lyons et

al., 2014). Regardless of the exact timing of origin, nitrogen fixation is believed to have arisen early in cyanobacteria, as phylogenetic evidence indicates that nitrogenase is an ancient, highly conserved enzyme complex that evolved before the rise of atmospheric oxygen levels 2.4 billion years ago (Broda and Peschek, 1983). Given these ancient developments, cyanobacteria could potentially offer insight into the past. Here, we have shown that *Anabaena cylindrica* strain PCC 7122 can record information about atmospheric N_2 levels in both its pattern of heterocyst formation as well as in its isotopic signature of nitrogen fixation. In the next two sections, we examine the potential of each response to serve as new geobarometers.

Heterocyst spacing as a paleoproxy for atmospheric N_2 levels

The quantifiable influence of N_2 partial pressure (pN_2) on heterocyst spacing is interesting from the perspective of understanding ancient atmospheric N_2 levels. Fossilized cyanobacteria with possible heterocysts have been arguably found in sedimentary rocks as old as 2 Ga (Fig. 15; Licari and Cloud, 1968) and convincingly found at the 400–million year (Ma) old Rhynie Chert of Scotland (Kidston and Lang, 1922); however, it is unclear whether heterocyst spacing in fossils such as these will be useful as a geobarometer for a variety of reasons.

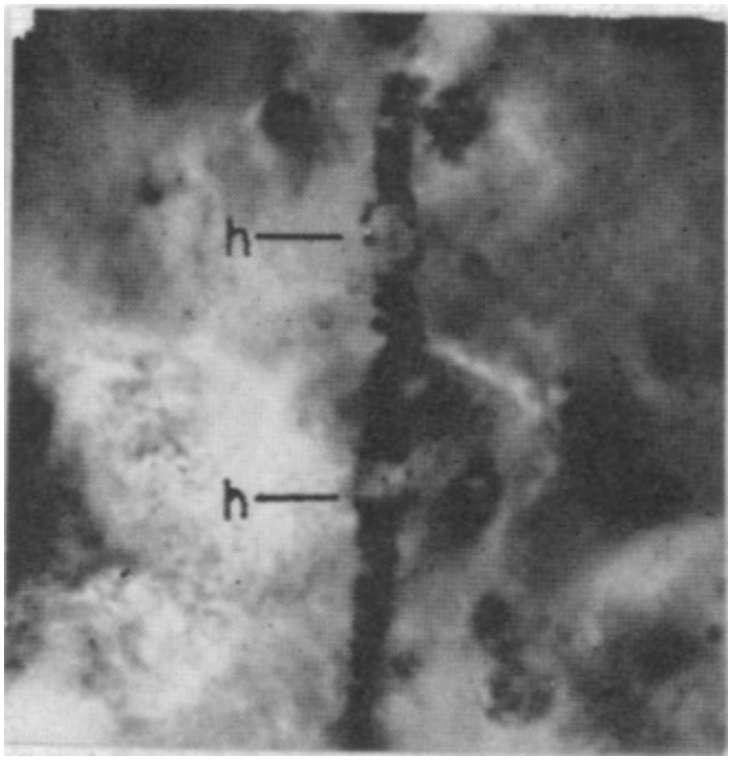

Figure 15. Fossilized cyanobacteria from the 1.9 billion year old Gunflint Iron Formation of southern Ontario with cells that appear to resemble heterocysts (h). Photograph taken from Licari and Cloud (1968).

The relationship between heterocyst distance and pN_2 is not absolute, as indicated by the wide distribution of interval lengths observed at each pN_2. This would make it difficult to extrapolate information about pN_2 unless a statistically significant number of samples could be collected from rocks, which is implausible given the low probability of an intact filament with at least two heterocysts fossilizing and remaining undisrupted for several billions of years. With current microscopy techniques that involve thin sectioning of rock samples, filaments must be oriented parallel to the thin section in order to be perserved during sample preparation, which increases the difficulty of obtaining intact filaments. However, new 3D microscopy techniques that do not require thin sectioning of rock samples may enable heterocystous filaments to be

found in larger volumes than permitted by thin sections, which could help circumvent other present challenges of finding fossilized cyanobacteria.

Despite future improvements in microscopy techniques, any potentially quantifiable relationship is further complicated by the fact that heterocyst spacing does not remain constant throughout culture growth, discrimination of which would be challenging. In addition, this effect appears to be limited to particular organisms, as *A. variabilis* did not respond to pN_2 in the same manner as *A. cylindrica*. Thus, differentiating between species in the rock record would be necessary, but also challenging. Finally, heterocystous cyanobacteria are believed to have evolved well after other cyanobacterial assemblages, as evident through phylogenetic analyses of 16S rRNAs from cyanobacteria (Giovannoni et al., 1988). Though this technique could not accurately date the evolution of heterocystous cyanobacteria due to the non-uniform rates of 16S rRNA mutation rates across species, it is clear that the extent in history to which this geobarometer can be applied is limited.

Ultimately, certain species of cyanobacteria may record atmospheric N_2 levels in their morphological features, but this response may not be useable to extrapolate environmental information from the rock record at this stage. Future research will explore the viability of this geobarometer.

Nitrogen isotope fractionation as a paleoproxy for atmospheric N_2 levels

The clear effect of pN_2 on the fractionation of isotopes during nitrogen fixation, coupled with the fact that numerous $\delta^{15}N$ values have been reported for sediments at various time points throughout Earth's history, confers a strong potential for nitrogen

isotope fractionation to serve as a paleoproxy for pN_2. The direct influence of pN_2 on $\delta^{15}N$ of biomass produced by nitrogenase has not yet been explored, but interpreting nitrogen isotope data from this perspective could lead to a greater understanding of ancient global nitrogen cycles. In the isotopic framework of our data coupled with current pN_2 constraints, organic matter deposited by *Anabaena* cyanobacteria would be expected to show more positive $\delta^{15}N$ values ~2.7 Ga (> –2‰) when surface atmospheric pressure was thought to be 0.23 ± 0.23 bar (Som et al., 2016), and increasingly negative $\delta^{15}N$ values leading up to the present as pN_2 increased to the 0.8 bar we see today.

Evidence for cyanobacterial activity in the rock record can be inferred from various cyanobacteria-specific biochemical indicators. In particular, the amphiphilic membrane lipids 2-methylhopanoids (Fig. 16) were once considered cyanobacterial biomarkers (Summons et al., 1999), and their discovery in Archean shales from the Pilbara Craton in Australia comprised controversial evidence for cyanobacterial existence ~2.7 Ga (Brocks et al., 1999). These amphiphilic membrane lipids are C2-methylated derivatives of bacteriohopanepolyols (BHPs), which are highly resistant to degradation due to their hydrocarbon composition, enabling them to be preserved and detected in fossils. However, 2-methylhopanoids do not contain nitrogen, so $\delta^{15}N$ information could not be extracted from these molecules. Furthermore, it is now known that BHPs are not exclusively found in cyanobacteria (Doughty et al., 2009; Ricci et al., 2013; Welander et al., 2010), complicating their use as a diagnostic.

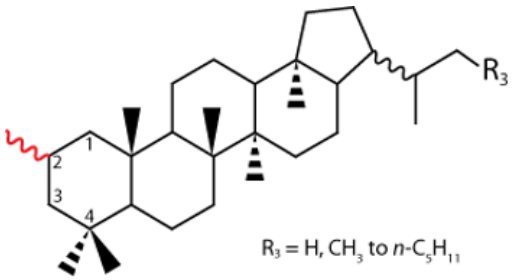

2-methylhopane

Figure 16. 2-methylhopanoids are derivatives of the membrane lipids bacteriohopanepolyols (BHPs) in which an extra methyl group has been added to C2 on one of the hydrocarbon rings. These molecules are more common to cyanobacteria than most other bacterial species, and were once believed to represent biomarkers for cyanobacteria.

The diagenetic products of chlorophyll breakdown include porphyrins (Fig. 17), which are preserved as stable geoporphyrins in sedimentary rock and contain δD, $\delta^{13}C$ and $\delta^{15}N$ isotopic information (Chikaraishi et al., 2005). These tetrapyrroles can be purified without disrupting the $\delta^{15}N$ content (Higgins et al., 2009) and could potentially serve as cyanobacterial biomarkers (Peters et al., 2007). Knowledge of other biomarkers is currently limited but must be explored in order to use $\delta^{15}N$ measurements from cyanobacteria nitrogen fixation products to quantify ancient N_2 partial pressure.

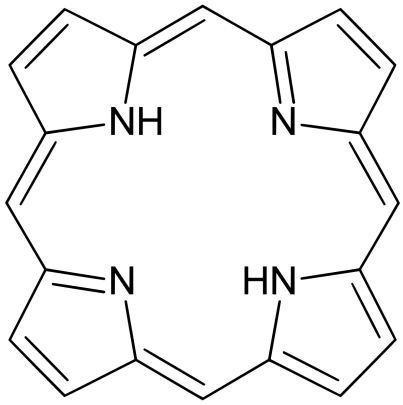

Figure 17. Porphyrins are breakdown products of chlorophyll in which the Mg^{2+} metal ion has been removed. Confined to photoautotrophic organisms, these tetrapyrroles preserve $\delta^{15}N$ information and may serve as biomarkers of cyanobacteria.

The isotope effects of nitrogen fixation and denitrification processes in the ocean largely contribute to the $\delta^{15}N$ of the global fixed nitrogen pool (Brandes and Devol, 2002; Deutsch et al., 2004). The nitrogen content of the modern ocean is dominated by nitrates, resulting in an average $\delta^{15}N$ of +5‰ (Liu and Kaplan, 1989; Liu et al., 1996; Sigman et al., 1999; Sigman et al., 1997). Nitrogen fixation by Mo-nitrogenase creates bioavailable nitrogen from N_2 at an isotopic composition of approximately –1‰, while preferential removal of the light isotope through denitrification leads to the enriched $\delta^{15}N$ (+5‰) of fixed oceanic nitrogen (Brandes and Devol, 2002). The wide range of $\delta^{15}N$ measurements from sediments from the Cretaceous Oceanic Anoxic Events (OAEs) and the Archean Eon has motivated extensive research seeking to understand ancient oceanic and atmospheric conditions that lead to these values, but to our knowledge, no interpretation of $\delta^{15}N$ has taken N_2 partial pressure into consideration for biomass from nitrogenase. Extremely low $\delta^{15}N$ values averaging –2‰ but reaching as low as –7‰ have been measured in Archean cherts (> 2.5 Ga) rich in kerogen (Pinti et al., 2001; Pinti et al., 2009; Beaumont and Robert, 1999; Thomazo and Papineau, 2013), and have

been linked to nitrogen fixation and other biological processes (Beaumont and Robert, 1999; Thomazo and Papineau, 2013). The $\delta^{15}N$ of N_2 in the Archean atmosphere was not substantially different from its modern value of 0‰ (Marty et al., 2013), so major differences in fractionation by nitrogenases in particular could be attributed to the fluctuating N_2 partial pressures over time. Sediments from the late Archean show more positive $\delta^{15}N$ (≥0‰), which has been considered a product of denitrification (Godfrey and Falkowski, 2009; Garvin et al., 2009). During this phase of the nitrogen cycle, fixed nitrogen is lost as nitrates are reduced to N_2, which can raise the oceanic $\delta^{15}N$ by as much as 6‰ (Brandes and Devol, 2002). In addition to this explanation, nitrogenases operating at this time under a low pN_2 could have partially contributed to this observed fractionation, which would support the current constraints of low atmospheric pressure (0.23 ± 0.23 bar) of the late Archean (Som et al., 2016).

The Cretaceous period is associated with several major OAEs characterized by brief (< 10^6 yr) but widespread marine seafloor anoxia, which led to the deposition of organic-rich sediments with characteristically low $\delta^{15}N$ values (+1.2 to –3.9‰) (Kuypers et al., 2004; Rau et al., 1987; Rigby and Batts, 1986). Various theories have attempted to reconcile these low nitrogen isotope ratios, including the idea that eukaryotes contributed substantially more biomass during these events than did cyanobacteria (Higgins et al., 2012), and that alternative nitrogenases (Fe and V) prevailed over Mo-nitrogenases during this nutrient-limited period of time (Zhang et al., 2014). This latter hypothesis is particularly interesting, as it maintains support for the significant contribution of nitrogen fixation to the nitrogen budget while providing an attractive explanation for the unusually low $\delta^{15}N$ values. Alternative nitrogenases

are expressed in certain cyanobacterial species such as *A. vinelandii* in Mo-limited conditions, and can drive the oceanic $\delta^{15}N$ to values as low as –7‰ (Zhang et al., 2014) whereas Mo-nitrogenases are not known to be capable of this.

The widespread anoxia during OAEs of the Cretaceous, Proterozoic and Archean time periods would have led to sulfide-rich reducing oceans (Jenkyns, 2010; Anbar and Knoll, 2002; Canfield, 1998), causing the geochemical depletion of molybdenum (Reinhard et al., 2013; Scott et al., 2008; Hetzel et al., 2009) and increase in iron bioavailability (Saito et al., 2003). Whether Mo-nitrogenase can be expressed in *A. cylindrica* without the presence of molybdenum is contested (Attridge and Rowell, 1997; Joerger et al., 1988), but it is generally believed that the euxinic, anoxic conditions during these OAEs would have favored a larger contribution to global nitrogen cycling by Fe-nitrogenases rather than Mo-nitrogenase (Anbar and Knoll, 2002; Zhang et al., 2014). For future studies, it would be interesting to examine how the isotope effects of both Mo-dependent and alternative nitrogenases are modulated by pN_2 in Mo-limited conditions. Such a study may more accurately induce cyanobacterial nitrogen fixation mechanisms that operated under ancient oceanic conditions, which could help elucidate the puzzling range of $\delta^{15}N$ values observed from these periods.

Acknowledgements

Sebastian Kopf

Sanjoy Som

Alexis Templeton

Templeton Lab

Kopf & Wing Lab

Richard Gordon

Brad Bebout

Leslie Bebout

Angela Detweiler

The Biological Sciences Initiative

Blue Marble Space Institute of Science

References

Anbar AD, Knoll AH. 2002. Proterozoic ocean chemistry and evolution: A bio-inorganic bridge? Science. 297:1137–1142.

Attridge EM, Rowell P. 1997. Growth, heterocyst differentiation and nitrogenase activity in the cyanobacteria *Anabaena variabilis* and *Anabaena cylindrica* in response to molybdenum and vanadium. New Phytol. 135:517-526.

Bauersachs T, Schouten S, Compaoré J, Wollenzien U, Stal LJ, Sinninghe Damsté JS. 2009. Nitrogen isotopic fractionation associated with growth on dinitrogen gas and nitrate by cyanobacteria. Limnol Oceanogr. 54:1403-1411.

Beaumont V, Robert F. 1999. Nitrogen isotope ratios of kerogens in Precambrian cherts: A record of the evolution of atmosphere chemistry? Precambrian Res 96:63–82.

Benson BB, Parker PDM. 1961. Nitrogen/argon and nitrogen isotope ratios in aerobic sea water. Deep-Sea Res. 7:237–253.

Berner RA. 2006. Geological nitrogen cycle and atmospheric N_2 over Phanerozoic time. Geochimica et Cosmochimica Acta. 65:685-694.

Brandes JA, Devol AH. 2002. A global marine-fixed nitrogen isotopic budget: Implications for Holocene nitrogen cycling. Global Biogeochem Cycles. 16:1-14.

Brocks JJ, Logan GA, Buick R, Summons RE. 1999. Archean molecular fossils and the early rise of eukaryotes. Science. 285:1033-1036.

Broda E, Peschek GA. 1983. Nitrogen fixation as evidence for the reducing nature of the early biosphere. Biosystems. 16:1-8.

Brown AI, Rutenberg AD. 2014. A storage-based model of heterocyst commitment and patterning in cyanobacteria. Phys Biol. 11:16001.

Brusca JS, Hale MA, Carrasco CD, Golden JW. 1989. Excision of an 11-kilobase-pair DNA element from within the *nifD* gene in *Anabaena variabilis* heterocysts. J Bacteriol. 171:4138–4145.

Buick R. 2008. When did oxygenic photosynthesis evolve? Phil Trans R Soc B. 363:2731-2743.

Buikema WJ, Haselkorn R. 1991. Characterization of a gene controlling heterocyst differentiation in the cyanobacterium *Anabaena* 7120. Genes Dev. 5:321–330.

Burris RH, Arp DJ, Benson DR, Emerich DW, Hagerman RV, Ljones T, Ludden PW, Sweet WJ. 1980. The biochemistry of nitrogenase, p. 37-54. In: Stewart WDP, Gallon JR, editors. Nitrogen fixation. Academic Press Ltd., London.

Callahan SM, Buikema SJ. 2001. The role of HetN in maintenance of the heterocyst pattern in *Anabaena* sp. PCC 7120. Mol Microbiol. 40:941-950.

Canfield DE. 1998. A new model for Proterozoic ocean chemistry. Nature. 396:450-453.

Cardemil L, Wolk CP. 1979. The polysaccharides from heterocyst and spore envelopes of a blue-green alga. Structure of the basic repeating unit. J Biol Chem. 254:736-741.

Cardona T, Styring S, Lindblad P, Magnuson A. 2008. Purified heterocysts from *Nostoc punctiforme* studied by laser scanning confocal microscopy, p. 755-758. In: JF Allen, E Gantt, JH Golbeck, B Osmond, editors. Photosynthesis: Energy from the Sun. 14th International Congress on Photosynthesis. Springer, Dordrecht, The Netherlands.

Carpenter EJ, Harvey HR, Fry B, Capone DG. 1997. Biogeochemical tracers of the marine cyanobacterium Trichodesmium. Deep Sea Res Part 1 Oceanogr Res. 44:27–38.

Chikaraishi Y, Matsumoto K, Ogawa NO, Suga H, Kitazato H, Ohkouchi N. 2005. Hydrogen, carbon and nitrogen isotopic fractionations during chlorophyll biosynthesis in C3 higher plants. Phytochemistry. 66: 911–920.

Cloud PE. 1973. Paleoecological significance of the banded iron-formation. Econ Geol. 68:1135-1143.

Codd GA, Stewart WDP. 1977. Ribulose-1,5-bisphosphate carboxylase in heterocysts and vegetative cells of *Anabaena cylindrica*. FEMS Microbiol Lett. 2:247-249.

Cornish-Bowden A. 1979. Fundamentals of enzyme kinetics. London, United Kingdom: Butterworths.

Deutsch C, Sigman DM, Thunell RC, Meckler AN, Haug GH. 2004. Isotopic constraints on glacial/interglacial changes in the oceanic nitrogen budget. Global Biogeochem Cycles. 18:1-22.

Dodd MS, Papineau D, Grenne T, Slack JF, Rittner M, Pirajno F, O'Neil J, Little CTS. 2017. Evidence for early life in Earth's oldest hydrothermal vent precipitates. Nature. 543:60-64.

Donze M, Haveman J, Scherick P. 1972. Absence of photosystem 2 in heterocysts of the blue-green alga *Anabaena*. Biochim Chiophys Acta. 256:157-161.

Doughty DM, Hunter RC, Summons RE, Newman DK. 2009. 2-Methylhopanoids are maximally produced in akinetes of *Nostoc punctiforme*: geobiological implications. Geobiology. 7:524–32.

Eisenhut M, Huege J, Schwarz D, Bauwe H, Kopka J, Hagemann M. 2008. Metabolome phenotyping of inorganic carbon limitation in cells of the wild type and photorespiratory mutants of the cyanobacterium *Synechocystis* sp. strain PCC 6803. Am Soc Plant Biol. 148:2109-2120.

Elhai J, Wolk CP. 1990. Developmental regulation and spatial pattern of expression of the structural genes for nitrogenase in the cyanobacterium *Anabaena*. EMBO J. 9:3379–3388.

Emerson S, Quay P, Stump C, Wilbur D, Knox M. 1991. O_2, Ar, N_2 and 222Rn in surface waters of the subarctic ocean: Net biological O_2 production. Glob Biogeochem Cycles 5:49–69.

Fay P, Cox RM. 1967. Oxygen inhibition of nitrogen fixation in cell-free preparations of blue-green algae. Biochim Chiophys Acta. 143:562-569.

Fay P. 1980. Nitrogen fixation in heterocysts, p. 121-165. In: Subba Rao NS, editors. Recent advances in biological nitrogen fixation. Edward Arnold, London.

Fay P. 1992. Oxygen relations of nitrogen fixation in cyanobacteria. Microbiol Rev. 56:340-373.

Fleming H, Haselkorn R. 1973. Differentiation in *Nostoc muscorum*: nitrogenase is synthesized in heterocysts. Proc Natl Acad Sci USA. 70:2727-2731.

Fleming H, Haselkorn R. 1974. The program of protein synthesis during heterocyst differentiation in nitrogen-fixing blue-green algae. Cell. 3:159-170.

Flores E, Herrero A, Wolk CP, Maldener I. 2006. Is the periplasm continuous in filamentous multicellular cyanobacteria? Trends Microbiol. 14:439-44.

Fogg GE, Stewart WDP, Fay P, Walsby AE. 1973. The blue-green algae. Science. 184:1066-1067.

Gallon JR. 1992. Reconciling the incompatible: N_2 fixation and O_2. New Phytol. 122:571–709.

Garrett TR, Bhakoo M, Zhang Z. 2008. Bacterial adhesion and biofilms on surfaces. Prog Nat Sci. 18:1049-1056.

Garvin J, Buick R, Anbar AD, Arnold GL, Kaufman AJ. 2009. Isotopic evidence for an aerobic nitrogen cycle in the latest Archean. Science. 323:1045–1048.

Giddings TH, Staehelin LA. 1981. Observation of microplasmodesmata in both heterocyst-forming and non-heterocyst-forming filamentous cyanobacteria by freeze-fracture electron microscopy. Arch Microbiol. 129:295-298.

Giovannoni SJ, Turner S, Olsen GT, Barns S, Lane DJ, Pace NR. 1988. Evolutionary relationships among cyanobacteria and green chloroplasts. J Bacteriol. 170:3584-3592.

Glazer AN. 1987. Phycobilisomes: assembly and attachment, p. 69-94. In: Fay P, Van Baalen C, editors. The cyanobacteria. Elsevier/Science Publishers B.V., Amsterdam.

Godfrey LV, Falkowski PG. 2009. The cycling and redox state of nitrogen in the Archaean ocean. Nat Geosci 2:725–729.

Goldblatt C, Claire M, Lenton T, Metthews A, Watson A, Zahnle K. 2009. Nitrogen-enhanced greenhouse warming on early Earth. Nat Geosci. 2:891-896.

Golden JW, Yoon HS. 2003. Heterocyst development in *Anabaena*. Curr Opin Microbiol. 6:557-563.

Gordon NK, Gordon R. 2016. How embryogenesis began in evolution, p. 1-74. In: Gordon NK, Gordon R, editors. Embryogenesis explained. World Scientific Publishing Company, Singapore.

Hallenbeck PC, Kostel PJ, Benemann JR. 1979. Purification and properties of nitrogenase from the cyanobacterium *Anabaena cylindrica*. Eur J Biochem. 98:275-284.

Haselkorn R. 1978. Heterocysts. Annu Rev Plant Physiol. 29:319-344.

Haselkorn R, Buikema WJ. 1992. Nitrogen fixation in cyanobacteria, p. 166-190. In: Stacey G, Burris RH, Evans HJ, editors. Biological Nitrogen Fixation. New York: Chapman & Hall.

Haury JF, Wolk CP. 1978. Classes of *Anabaena variabilis* mutants with oxygen-sensitive nitrogenase activity. J Bacteriol. 136:688-692.

Hayes JM. 2004. An introduction to isotopic calculations. Atomic Energy. 1-10.

Herrero A, Muro-Pastor AM, Valladares A, Flores E. 2004. Cellular differentiation and the NtcA transcription factor in filamentous cyanobacteria. FEMS Microbiol Rev. 28:469-487.

Herrero A, Wolk CP. 1986. Genetic mapping of the chromosome of the cyanobacterium, *Anabaena variabilis*. Proximity of the structural genes for nitrogenase and ribulose-bisphosphate carboxylase. J Biol Chem. 261: 7748–7754.

Hetzel A, Böttcher ME, Wortmann UG, Brumsack H-J. 2009. Paleo-redox conditions during OAE 2 reflected in Demerara Rise sediment geochemistry (ODP Leg 207). Palaeogeogr Palaeoclimatol Palaeoecol. 273:302-328.

Higgins MB, Robinson RS, Casciotti KL, McIlvin MR, Pearson A. 2009. A method for determining the nitrogen isotopic composition of porphyrins. Anal Chem. 81:184-192.

Higgins MB, Robinson RS, Husson JM, Carter SJ, Pearson A. 2012. Dominant eukaryotic export production during ocean anoxic events reflects the importance of recycled NH_4^+. 109:2269-2274.

Holland HD. 2006. The oxygenation of the atmosphere and oceans. Phil Trans R Soc B. 361:903–915.

Igarishi RY, Seefeldt L. 2003. Nitrogen fixation: the mechanism of the Mo-dependent nitrogenase. Crc Cr Rev Bioch Mol. 38:351-384.

Jenkyns HC. 2010. Geochemistry of oceanic anoxic events. Geochem Geophy Geosy. 11:Q03004.

Joerger RD, Bishop PE, Evans HJ. 1988. Bacterial alternative nitrogen fixation systems. CRC Crit Rev Microbiol. 16:1-14.

Kidston R, Lang WH. 1922. On Old Red Sandstone plants showing structure from the Rhynie chert bed, Aberdeenshire, part V. Trans R Soc Edinb. 52:885–902.

Knight MR, Campbell AK, Smith SM, Trewavas AJ. 1991. Recombinant aequorin as a probe for cytosolic free Ca^{2+} in Escherichia coli. FEBS Lett. 282:405–408.

Komárek J, Anagnostidis KK. 1989. Modern approach to the classification system of Cyanophytes 4 – Nostocales. Int J Phyc Res. 82:247-345.

Kopp RE, Kirschvink JL, Hilburn IA, Nash CZ. 2005.The Paleoproterozoic snowball Earth: a climate disaster triggered by the evolution of oxygenic photosynthesis. Proc Nat Acad Sci. 102:11131–11136.

Kulasooriya SA, Lang NJ, Fay P. 1972. The heterocysts of blue-green algae. III. Differentiation and nitrogenase activity. Proc R Soc London Ser B. 181:199-209.

Kumar K, Mella-Herrera RA, Golden JW. 2010. Cyanobacterial heterocysts. Cold Spring Harb Perspect Biol. 2:1-19.

Kump LR. 2008. The rise of atmospheric oxygen. Nature. 451:277-278.

Kuypers MMM, van Breugel Y, Schouten S, Erba E, Damsté JSS. 2004. N_2-fixing cyanobacteria supplied nutrient N for Cretaceous oceanic anoxic events. Geology. 32:853–856.

Lambein F, Wolk CP. 1973. Structural studies on the glycolipids from the envelope of the heterocyst of *Anabaena cylindrica*. Biochemistry 12:791-798.

Lang NJ, Fay P. 1971. The heterocysts of blue-green algae II. Details of ultrastructure. Proc R Soc London Ser B. 178:193-203.

Laurent S, Chen H, Bedu S, Ziarelli F, Peng L, Zhang C. 2001. Nonmetabolizable analogue of 2-oxoglutarate elicits heterocyst differentiation under repressive conditions in *Anabaena* sp. PCC 7120. Arch Microbiol. 176:9-18.

Licari GR, Cloud PE. 1968. Reproductive structures and taxonomic affinities of some nannofossils from the Gunflint Iron Formation. Proc Nat Acad Sci. 59:1053-1060.

Liu KK, Kaplan IR. 1989. The Eastern Tropical Pacific as a source of N-15-enriched nitrate in seawater off southern-California, Limnol Oceanogr. 34:820–830.

Liu KK, Su MJ, Hsueh CR, Gong GC. 1996. The nitrogen isotopic composition of nitrate in the Kuroshio Water northeast of Taiwan: Evidence for nitrogen fixation as a source of isotopically light nitrate. Mar Chem. 54:273–292.

Lyons TW, Reinhard CT, Planavsky NJ. 2014. The rise of oxygen in Earth's early ocean and atmosphere. Nature. 506:307–15.

Mariscal V, Herrero A, Flores E. 2007. Continuous periplasm in a filamentous, heterocyst-forming cyanobacterium. Mol Microbiol. 65:1139-1145.

Marty B, Zimmermann L, Pujol M, Burgess R, Philippot P. 2013. Nitrogen isotopic composition and density of the Archaean atmosphere. Science. 342:101-104.

Meeks JC, Elhai J. 2002. Regulation of cellular differentiation in filamentous cyanobacteria in free-living and plant-associated symbiotic growth states. Microbiol Mol Bio Rev. 66:94-121.

Meeks JC, Wolk CP, Lockau W, Schilling N, Shaffer PW, Chien WS. 1978. Pathways of assimilation of $[^{12}N]N_2$ and $[^{12}NH_4]$ by cyanobacteria with and without heterocysts. J Bacteriol. 134:125-130.

Minagawa M, Wada E. 1986. Nitrogen isotopes ratios of red tide organisms in the East China sea: A characterization of biological nitrogen fixation. Mar Chem 19:245–259.

Mortenson LE, Thorneley RNF. 1979. Structure and function of nitrogenase. Annu Rev Biochem. 48:387-418.

Muro-Pastor AM, Reyes JC, Florencio FJ. 2001. Cyanobacteria perceive nitrogen status by sensing intracellular 2-oxoglutarate levels. J Biol Chem. 276:38320-38328.

Murry MA, Wolk CP. 1989. Evidence that the barrier to the penetration of oxygen into heterocysts depends upon two layers of the cell envelope. Arch Microbiol. 151:469-474.

Ohmori M, Hattori A. 1972. Effect of nitrate on nitrogen-fixation by the blue-green alga *Anabaena cylindrica*. Plant & Cell Physiol. 13:589–599.

Onek LA, Smith RJ. 1992. Calmodulin and calcium mediated regulation in prokaryotes. J Gen Microbiol 138:1039–1049.

Paerl HW. 1978. Role of heterotrophic bacteria in promoting N_2 fixation by Anabaena in aquatic habitats. Microb Ecol. 4:215-231.

Peters KE, Walters CC, Moldowan JM. 2007. Biochemistry of biomarkers, p. 45-71. In: Peters KE, Walters CC, Moldowan JM, editors. Cambridge University Press. The biomarker guide: Biomarkers and isotopes in the environment and human history.

Pinti DL, Hashizume K, Matsuda J. 2001. Nitrogen and argon signatures in 3.8 to 2.8 Ga metasediments: Clues on the chemical state of the Archean ocean and the deep biosphere. Geochim Cosmochim Acta. 65:2301–2315.

Pinti DL, Hashizume K, Sugihara A, Massault M, Philippot P. 2009. Isotopic fractionation of nitrogen and carbon in Paleoarchean cherts from Pilbara craton, Western Australia: Origin of 15N-depleted nitrogen. Geochim Cosmochim Acta. 73:3819–3848.

Rau GH, Arthur MA, Dean WE. 1987. $^{15}N/^{14}N$ variations in Cretaceous Atlantic sedimentary sequences: Implications for past changes in marine nitrogen biogeochemistry. Earth Planet Sci Lett. 82:269–279.

Reinhard CT, Planavsky NJ, Robbins LJ, Partin CA, Gill BC, Lalonde SV, Bekker A, Konhauser KO, Lyons TW. 2013. Proterozoic ocean redox and biogeochemical stasis. Proc Natl Acad Sci USA. 110:5357-5362.

Ricci JN, Coleman ML, Welander PV, Sessions AL, Summons RE, Spear JR, Newman DK. 2013. Diverse capacity for 2-methylhopanoid production correlates with a specific ecological niche. ISME J. 8:675–684.

Rigby D, Batts BD. 1986. The isotopic composition of nitrogen in Australian coals and oil shales. Chem Geol. 58:273–282.

Rippka R, Deruelles J, Waterbury JB, Herdman M, Stanier RY. 1979. Generic assignments, strain histories and properties of pure cultures of cyanobacteria. J Gen Microbiol. 111:1-61.

Risser DD, Wong FCY, Meeks JC. 2012. Biased inheritance of the protein PatN frees vegetative cells to initiate patterned heterocyst differentiation. Proc Nat Acad Sci. 109:15342-15347.

Robson RL, Postgate JR. 1980. Oxygen and hydrogen in biological nitrogen fixation. Annu Rev Microbiol. 34:183-207.

Saito MA, Sigman DM, Morel FMM. 2003. The bioinorganic chemistry of the ancient ocean: The co-evolution of cyanobacterial metal requirements and biogeochemical cycles at the Archean-Proterozoic boundary? Inorg Chim Acta. 356:308–318.

Sander R. 2015. Compilation of Henry's law constants (version 4.0) for water as solvent. Atmos Chem Phys. 15:4399-4981.

Schoeller DA. 1999. Isotope fractionation: Why aren't we what we eat? J Arachaeol Sci. 26:667-673.

Schopf JW. 1993. Microfossils of the early Archean Apex chert: new evidence of the antiquity of life. Science. 260:640-646.

Schopf JW, Walter MR. 1982. Origin and early evolution of cyanobacteria: the geological evidence, p. 543-564. In: Carr NG, Whitton BA, editors. The biology of cyanobacteria. Blackwell Scientific Publications Ltd., Oxford.

Schrautemeier B, Neveling U, Schmitz S. 1995. Distinct and differently regulated Mo-dependent nitrogen-fixing systems evolved for heterocysts and vegetative cells of *Anabaena variabilis* ATCC 29413—characterization of the *fdxH1/2* gene regions as part of the *nif1/2* gene clusters. Mol Microbiol. 18:357–369.

Scott C, Lyons TW, Bekker A, Shen Y, Poulton SW, Chu X, Anbar AD. 2008. Tracing the stepwise oxygenation of the Proterozoic ocean. Nature. 452:456-459.

Shi Y, Zhao W, Zhang W, Ye Z, Zhao J. 2006. Regulation of intracellular free calcium concentration during heterocyst differentiation by HetR and NtcA in *Anabaena* sp. PCC 7120. Proc Natl Acad Sci USA. 103:11334-11339.

Sigman, DM, Altabet MA, McCorkle DC, Francois R, Fischer G. 1999. The delta N-15 of nitrate in the Southern Ocean: Consumption of nitrate in surface waters. Global Biogeochem Cycles. 13:1149–1166.

Sigman, DM, Altabet MA, Michener R, McCorkle DC, Fry B, Holmes RM. 1997. Natural abundance-level measurement of the nitrogen isotopic composition of oceanic nitrate: An adaptation of the ammonia diffusion method. Mar Chem. 57:227–242.

Smith RJ, Hobson S, Ellis IR. 1987. Evidence for calcium-mediated regulation of heterocyst frequency and nitrogenase activity in *Nostoc* 6720. New Phytol. 105:531–541.

Smith RJ, Wilkins A. 1988. A correlation between intracellular calcium and incident irradiance in *Nostoc* 6720. New Phytol. 109:157–161.

Som SM, Buick R, Hagadorn JW, Blake TS, Perreault JM, Harnmeijer JP, Catling DC. 2016. Earth's air pressure 2.7 billion years ago constrained to less than half of modern levels. Nat Geosci. 9:1–5.

Som SM, Catling DC, Harnmeijer JP, Polivka PM, Buick R. 2012. Air density 2.7 billion years ago limited to less than twice modern levels by fossil raindrop imprints. Nature. 484:359–362.

Sra A, Hu Y, Martin G, Snow D, Ribbe M, Kohen A. 2004. Competitive ^{15}N kinetic isotope effects of nitrogen-catalyzed dinitrogen reduction. J Am Chem Soc. 126:12768–12769.

Stanier RY, Cohen-Bazire G. 1977. Phototrophic prokaryotes: the cyanobacteria. Ann Rev Microbiol. 31:225-274.

Stewart WDP, Rowell P, Tel-Or E. 1975. Nitrogen fixation and the heterocyst in blue-green algae. Biochem Soc Trans. 3:357-361.

Stüeken EE, Kipp MA, Koehler MC, Schwieterman EW, Johnson B, Buick R. 2016. Modeling pN_2 through geological time: Implications for planetary climates and atmospheric biosignatures. 16:949-963.

Summons RE, Jahnke LL, Hope JM, Logan GA. 1999. 2-Methylhopanoids as biomarkers for cyanobacterial oxygenic photosynthesis. Nature. 400:554-557.

Tel-Or E, Stewart WDP. 1975. Manganese and photosynthetic oxygen evolution by algae. Nature. 258:715-716.

Tel-Or E, Stewart WDP. 1977. Photosynthetic components and activities of nitrogen-fixing isolated heterocysts of *Anabaena cylindrica*. Proc R Soc London Ser B. 198:61-86.

Temple SJ, Vance CP, Gantt JS. 1998. Glutamate synthase and nitrogen assimilation. Trends Plant Sci. 3:51-56.

Thiel T. 1993. Characterization of genes for an alternative nitrogenase in the cyanobacterium *Anabaena variabilis*. J Bacteriol. 175:6276-6286.

Thiel T, Lyons EM, Erker JC, Ernst A. 1995. A second nitrogenase in vegetative cells of a heterocyst-forming cyanobacterium. Proc Natl Acad Sci USA. 92:9358-9362.

Thiel T, Lyons EM, Erker JC. 1997. Characterization of genes for a second Mo-dependent nitrogenase in the cyanobacterium *Anabaena variabilis*. J Bacteriol. 179:5222–5225.

Thiel T, Pratte B. 2001. Effect on heterocyst differentiation of nitrogen fixation in vegetative cells of the cyanobacterium *Anabaena variabilis* ATCC 29413. J Bacteriol. 183:280-286.

Thomas J. 1970. Absence of the pigments of photosystem II of photosynthesis in heterocysts of a blue-green alga. Nat Lond. 228:181-183.

Thomas J, Meeks JC, Wolk CP, Shaffer PW, Austin SM, Chien W-S. 1977. Formation of glutamine from [13N]ammonia, [13N]dinitrogen, and [14C]glutamate by heterocysts isolated from Anabaena cylindrica. J Bacteriol. 129:15435–1555.

Thomazo C, Papineau D. 2013. Biogeochemical cycling of nitrogen on the early Earth. Elements. 9:345–351.

Torrecilla I, Leganés F, Bonilla I, Fernández-Piñas F. 2004. A calcium signal is involved in heterocyst differentiation in the cyanobacterium *Anabaena* sp. PCC7120. Microbiol. 150:3731–3739.

Unkovich M. 2013. Isotope discrimination provides new insight into biological nitrogen fixation. New Phytol. 198:643-646.

Walsby AE. 1967. Mucilage secretion and the movements of blue-green algae. Protoplasma. 65:223-238.

Walsby AE. 1985. The permeability of heterocysts to the gases nitrogen and oxygen. Proc R Soc London Ser B. 226:345-367.

Walsby AE. 2007. Cyanobacterial heterocysts: terminal pores proposed as sites of gas exchange. Trends Microbiol. 15:340-349.

Ward B. 2012. The global nitrogen cycle. Fund Geobio. 1:36-48.

Ward LM, Kirschvink JL, Fischer WW. 2015. Timescales of oxygenation following the evolution of oxygenic photosynthesis. Orig Life Evol Biospheres. 46:51–65.

Welander PV, Coleman ML, Sessions AL, Summons RE, Newman DK. 2010. Identification of a methylase required for 2-methylhopanoid production and implications for the interpretation of sedimentary hopanes. Proc Nat Acad Sci. 107:8537–8542

Wilcox M, Mitchison GJ, Smith RJ. 1973. Pattern formation in the blue-green alga *Anabaena*. J Cell Sci. 12:707-723.

Winkenbach F, Wolk CP, Jost M. 1972. Lipids of membranes and of the cell envelope in heterocysts of a blue-green alga. Planta. 107:69-80.

Winkenbach F, Wolk CP. 1973. Activities of enzymes of the oxidative and reductive pentose phosphate pathways in heterocysts of a blue-green alga. Plant Physiol. 52:480-483.

Wolk CP, Cai Y, Cardemil L, Flores E, Hohn B, Murry M, Schmetterer G, Schrautemeier B, Wilson R. 1988. Isolation and complementation of mutants of *Anabaena* sp. strain PCC7120 unable to grow aerobically on dinitrogen. J Bacteriol. 170:1239-1244.

Wolk CP, Ernst A, Elhai J. 1994. Heterocyst metabolism and development. p. 769-823. In: Bryant DA, editors. The molecular biology of cyanobacteria, vol. 1. Kluwer Academic Publishers, Dordrecht, The Netherlands.

Wolk CP. 1965. Heterocyst germination under defined conditions. Nature. 205:201-202.

Wolk CP. 1967. Physiological basis of the pattern of vegetative growth of a blue-green alga. Proc Natl Acad Sci. 57:1246-1251.

Wolk CP. 1968. Movement of carbon from vegetative cells to heterocysts in *Anabaena cylindrica*. J Bacteriol. 96:2138-2143.

Wolk CP, Simon RD. 1969. Pigments and lipids of heterocysts. Planta. 86:92-97.

Wolk CP. 1989. Alternative models for the development of the pattern of spaced heterocysts in *Anabaena* (*Cyanophyta*). Plant Syst Evol. 164:27-31.

Wood NB, Haselkorn R. 1976. Protein degradation during heterocyst development in *Anabaena*, p. 125-127. In: Codd GA, Stewart WDP, editors. Proc. 2nd Int. Symp. Photosynth. Prokaryotes, Dundee, Scotland.

Yoon HS, Golden JW. 1998. Heterocyst pattern formation controlled by a diffusible peptide. Science. 282:935-938.

Yoon HS, Golden JW. 2001. PatS and products of nitrogen fixation control heterocyst pattern. J Bacteriol. 183:2605–2613.

Zhang C, Laurent S, Sakr S. 2006. Heterocyst differentiation and pattern formation in cyanobacteria: a chorus of signals. Mol Microbiol. 59:367-375.

Zhang X, Sigman DM, Morel, FMM, Kraepiel AML. 2014. Nitrogen isotope fractionation by alternative nitrogenases and past ocean anoxia. Proc Natl Acad Sci. USA. 111:4782-4787.

Zhao J, LaClaire JW, Brand JJ. 1991. Calcium and heterocyst development in *Anabaena* 7120, p. 105. In: Abstracts of the VII International Symposium on Photosynthetic Prokaryotes. University of Massachusetts, Amherst, USA.

Zhao Y, Shi Y, Zhao W, Huang X, Wang D, Brown N et al. 2005. CcbP, a calcium-binding protein from *Anabaena* sp. PCC 7120, provides evidence that calcium ions regulate heterocyst differentiation. Proc Natl Acad Sci USA. 102:5744-5748.

Appendices

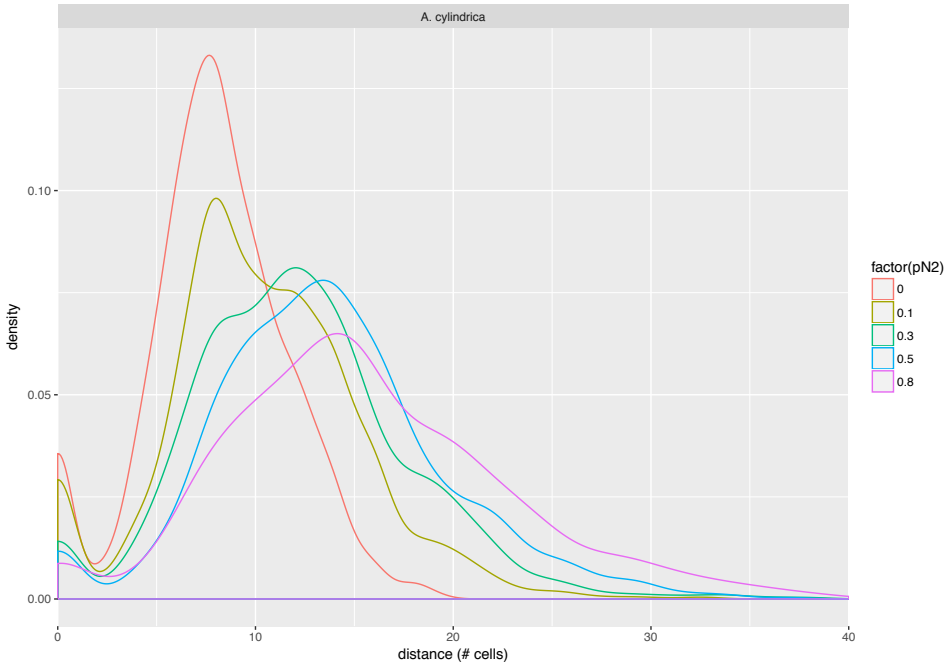

Figure S1. Distribution of heterocyst spacing for *Anabaena cylindrica* PCC 7122 grown under different pN_2.

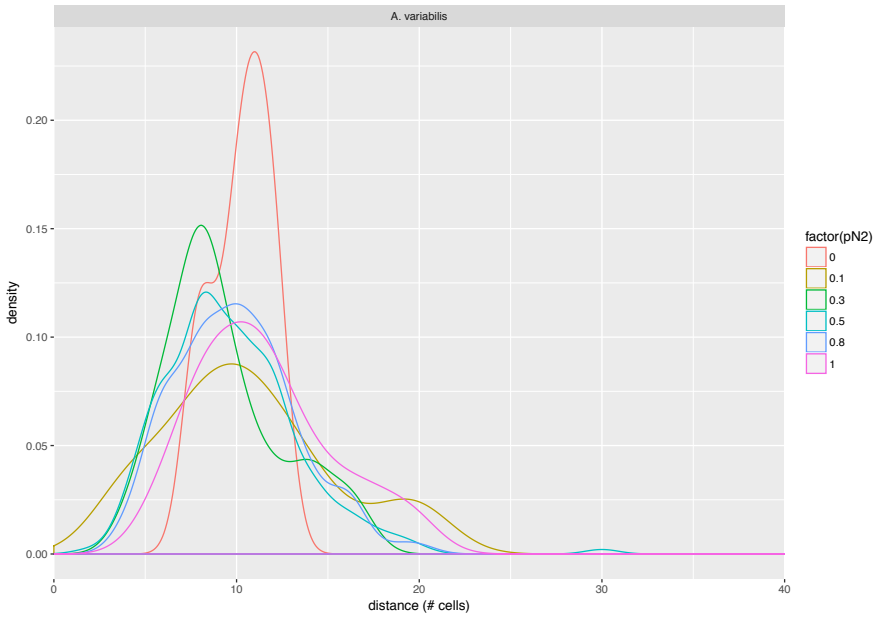

Figure S2. Distribution of heterocyst spacing for *Anabaena variabilis* ATCC 29413 grown under different pN_2.

Table S1. *Anabaena cylindrica* PCC 7122 heterocyst distances in response to N_2 partial pressure, including and excluding contiguous heterocyst intervals.

	with contiguous heterocysts *(# cells)*			without contiguous heterocysts *(# cells)*		
$\mathbf{pN_2}$ *(bar)*	$\bar{x}_{\mathbf{het}}$	$\mathbf{M_{het}}$	$\mathbf{1\sigma}$	$\bar{x}_{\mathbf{het}}$	$\mathbf{M_{het}}$	$\mathbf{1\sigma}$
0	8.0	8	3.6	8.6	8	3.0
0.1	10.2	10	4.9	10.9	10	4.3
0.3	12.1	12	5.5	12.6	12	5.0
0.5	13.7	13	5.9	14.12	14	5.5
0.8	15.6	15	7.5	16.11	15	7.0

Comparison of heterocyst distance measurements for *Anabaena cylindrica* in response to pN_2 when contiguous heterocyst intervals were included (left) and excluded (right) in the cell counts. Results are reported as: mean ($\bar{x}_{het}$), median (M_{het}) and one standard deviation (1σ), and did not vary significantly between the two methods of computation.

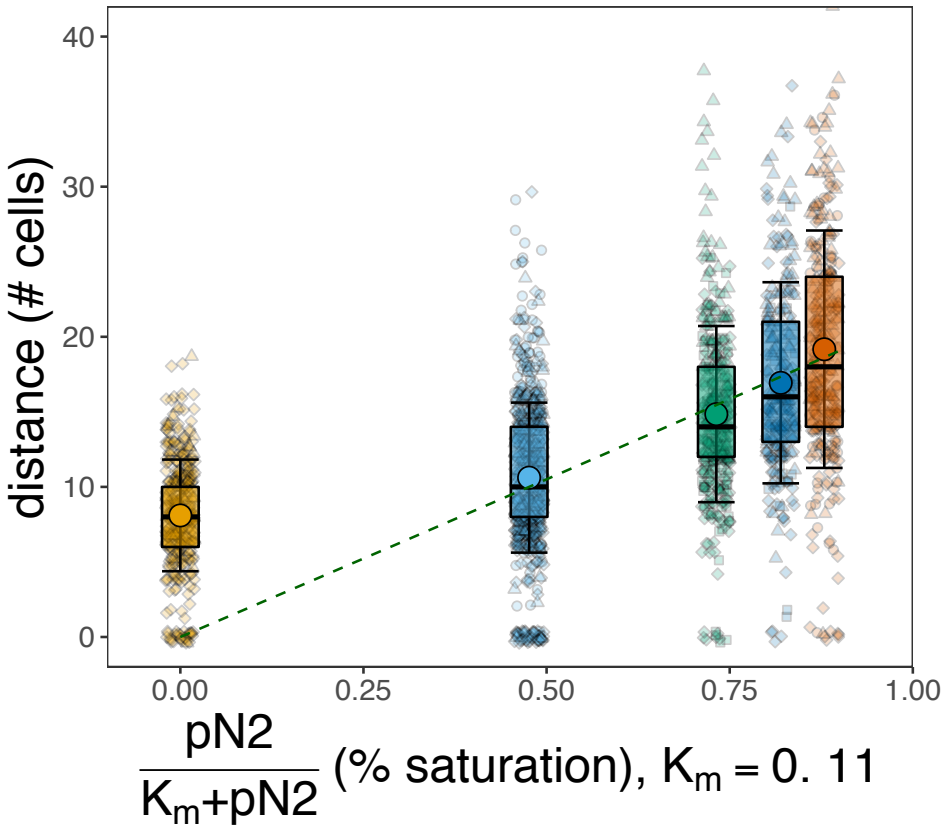

Figure S3. *Anabaena cylindrica* PCC 7122 heterocyst distance data from Figure 7, plotted against nitrogen fixation rates to reflect enzyme kinetics involved in heterocyst spacing. The half-saturation constant K_M was optimized by residual analysis and the resulting value of 0.11 ± 0.013 bar N_2 was used to fit the linear plot.

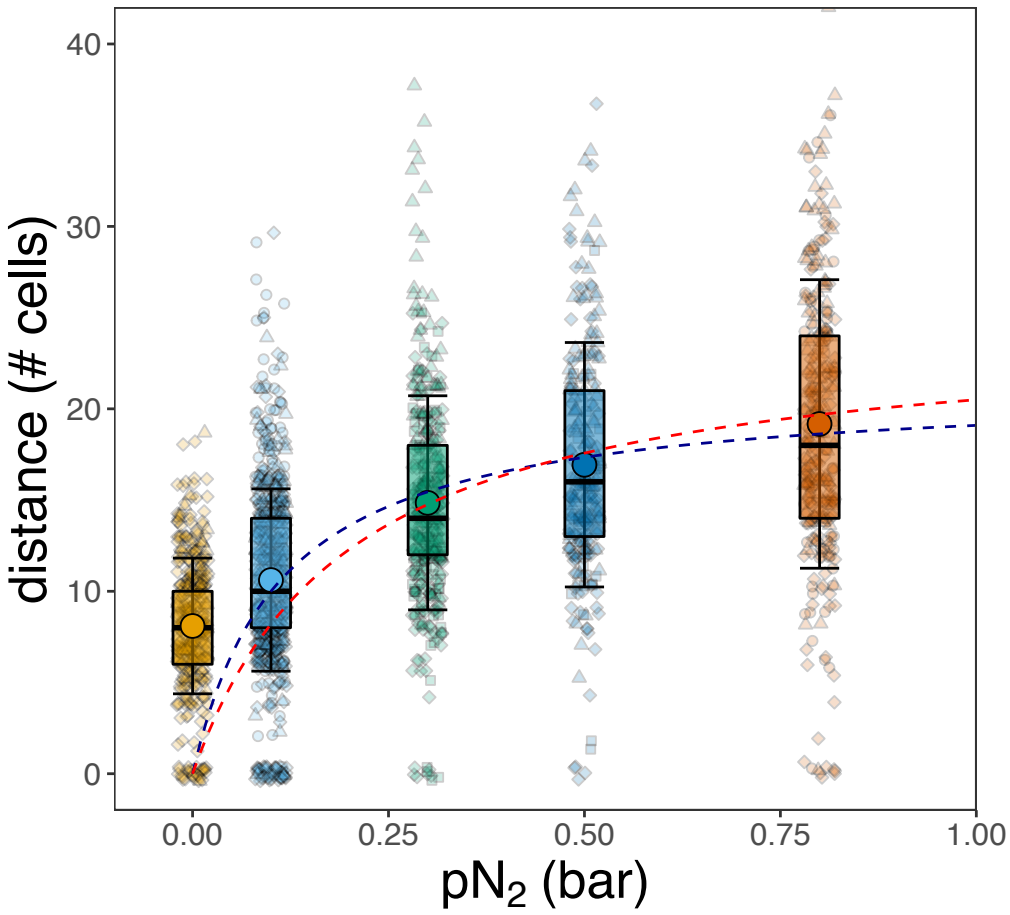

Figure S4. *Anabaena cylindrica* PCC 7122 heterocyst distance data from Figure 7. A nonlinear least squares fit following the Michaelis-Menten model of enzyme kinetics (Eq. 3) was plotted with a forced calibration through zero using the inferred half-saturation constant K_M of 0.11 ± 0.013 bar N_2 from Fig. S3 (dashed blue). A previously estimated K_M of 0.2 (Ohmori and Hattori, 1972) for *A. cylindrica* nitrogenase was used to generate a second curve following the same approach (red dashed).

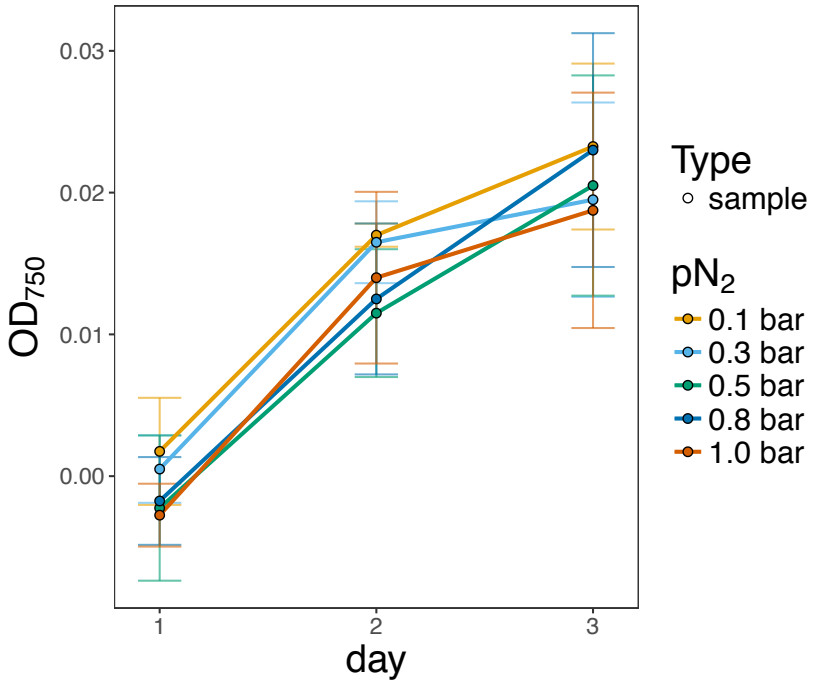

Figure S5A. Experiment 1: Growth of *Anabaena variabilis* ATCC 29413 under different pN_2. OD_{750} measurements were taken daily for 3 days.

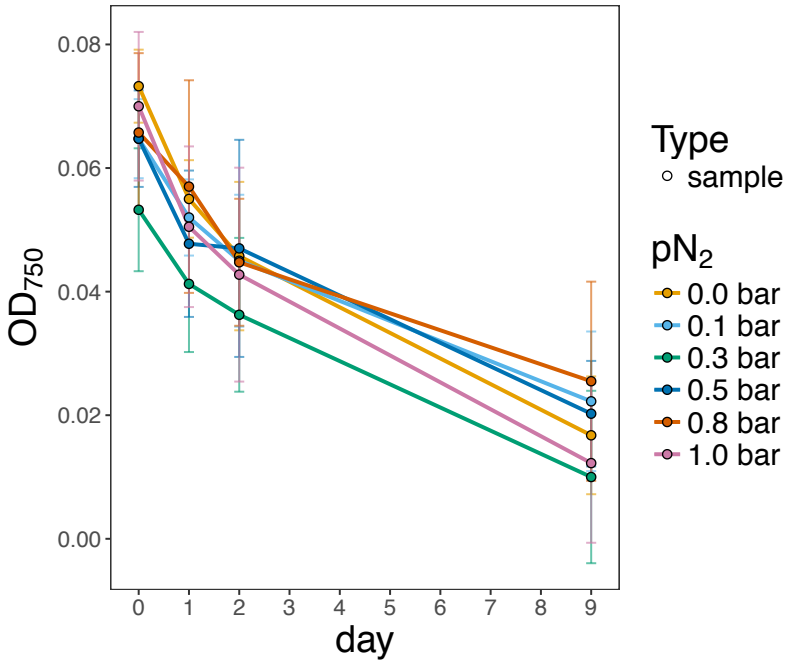

Figure S5B. Experiment 2: Growth of *Anabaena variabilis* ATCC 29413 under different pN_2. OD_{750} measurements were taken daily for 10 days.

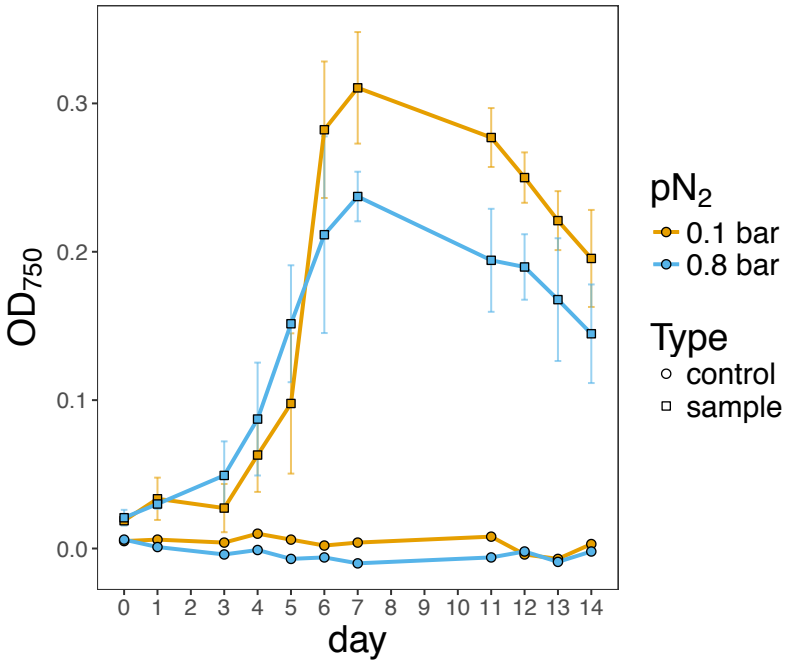

Figure S5C. Experiment 3: Growth of *Anabaena cylindrica* PCC 7122 under different pN_2. OD_{750} measurements were taken daily for 15 days.

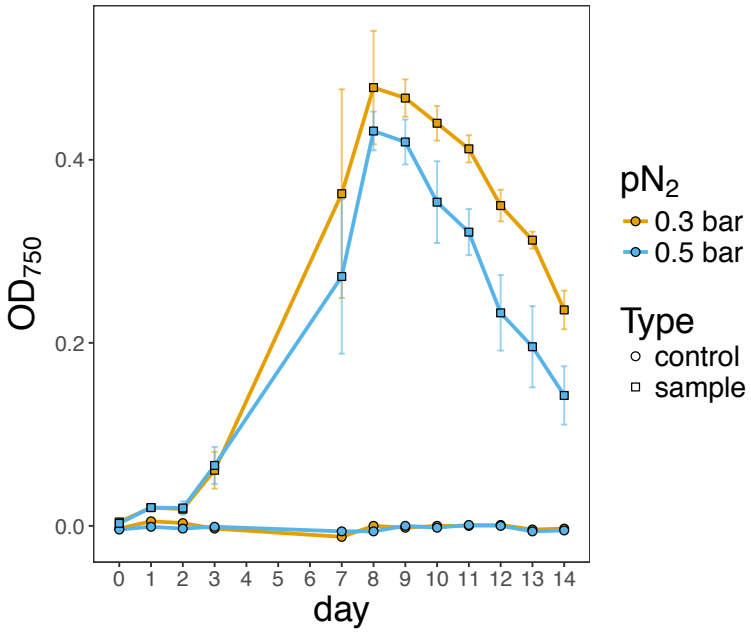

Figure S5D. Experiment 4: Growth of *Anabaena cylindrica* PCC 7122 under different pN_2. OD_{750} measurements were taken daily for 15 days.

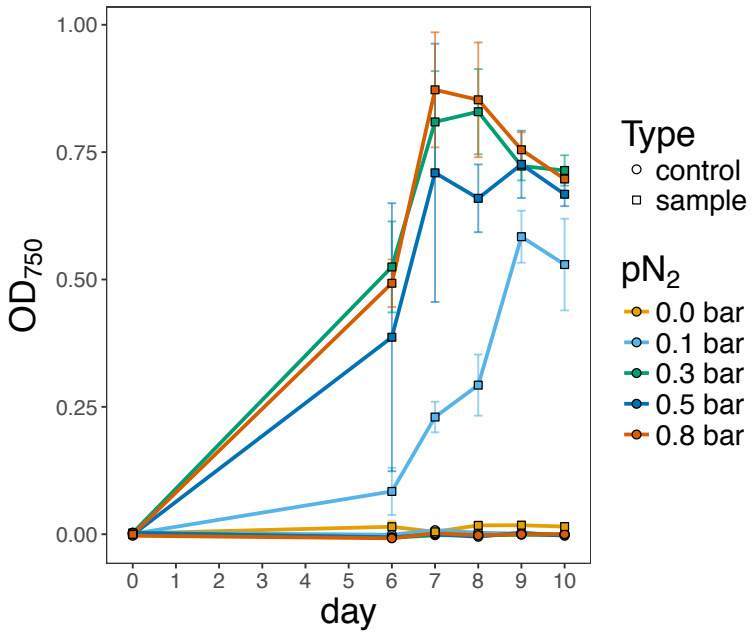

Figure S5E. Experiment 5: Growth of *Anabaena cylindrica* PCC 7122 under different pN_2. OD_{750} measurements were taken daily for 11 days.